USING TREE-RING GROWTH AND STABLE ISOTOPES TO EXPLORE PONDEROSA PINE ECOPHYSIOLOGICAL RESPONSES TO CLIMATE VARIABILITY AND THE 2012-2015 CALIFORNIA DROUGHT

by

Rachel M. Keen

A thesis submitted in partial fulfillment
of the requirements for the degree

of

MASTER OF SCIENCE

in

Ecology

Approved:

_____	_____
Steve L. Voelker, Ph.D. Major Professor	Barbara J. Bentz, Ph.D. Committee Member
_____	_____
Simon Wang, Ph.D. Committee Member	Richard S. Inouye, Ph.D. Vice Provost for Graduate Studies

UTAH STATE UNIVERSITY
Logan, Utah

2019

ABSTRACT

Using Tree-Ring Growth and Stable Isotopes to Explore Ponderosa Pine Ecophysiological Responses to Climate Variability and the 2012-2015 California Drought

by

Rachel M. Keen, Master of Science

Utah State University, 2019

Major Professor: Steve L. Voelker
Department: Plants, Soils and Climate

As the climate continues to warm, forests in the western United States are being subject to more frequent and severe drought events, making it increasingly important to understand how trees respond to drought stress. The 2012-2015 California drought, is a recent example of an extreme drought event coupled with an epidemic scale bark beetle outbreak that led to widespread mortality of ponderosa pine. In these studies, we utilized tree-ring growth and stable isotopes to better understand (1) whether drought stress affected local-scale variability in survival of ponderosa pines during an epidemic outbreak of western pine beetle and (2) to what extent important ecosystem carbon and water fluxes were recorded in ponderosa pine tree-rings during this severe drought event. In the first portion of this study, increment cores from pairs of surviving and dead ponderosa pines in the southern Sierra Nevadas were collected after the drought event to compare growth rates and tree-ring stable isotopes. Our goal was to determine whether

increased drought stress was associated with higher susceptibility to beetle attack and, consequently, mortality. Unexpectedly, we found no stable isotope evidence for more severe drought stress in trees that died. Instead, we found that surviving trees grew consistently faster from 1900-2016. Our results suggest that differences in growth rate had more influence on susceptibility to beetle attack than severity of drought stress. In the second portion of this study, we used intra-annual growth and stable isotope measurements to explore the relationship between tree-level and ecosystem-level carbon and water fluxes during the same drought event. Our results showed that tree-level water use efficiency had a strong negative relationship with ecosystem-scale water use efficiency measured at an on-site flux tower, likely due to the impact of soil and stream water evaporation on flux tower measurements of evapotranspiration. Additionally, tree-ring growth rates had a strong positive relationship with ecosystem-scale gross primary productivity. Using tree-ring stable isotopes and growth rates as proxies for water use efficiency and gross primary productivity, respectively, we were able to accurately predict ecosystem-scale ET using tree-level measurements during the 2012-2015 drought event.

(123 pages)

PUBLIC ABSTRACT

Using Tree-Ring Growth and Stable Isotopes to Explore Ponderosa Pine Ecophysiological Responses to Climate Variability and the 2012-2015 California Drought

Rachel M. Keen

Climate warming in recent decades has resulted in more frequent and severe drought events in the western United States. These changes are projected to continue, making it exceedingly important to understand how forests respond to severe drought stress, and how we can manage these forests to reduce mortality during future events. The 2012-2015 California drought is a recent example of a severe, multi-year drought that was coupled with an epidemic-scale outbreak of western pine beetle, killing nearly 90% of ponderosa pines in the central and southern Sierra Nevadas. In the first portion of this study, we compared pairs of surviving and dead ponderosa pines following this drought event to determine how the surviving trees were able to survive. We were also interested in how closely ponderosa pine tree-rings were recording ecosystem responses to this drought event. In the second portion of this study, we compared tree-ring growth rates and stable isotopes to data from an on-site flux tower to determine whether tree-rings were recording important information regarding ecosystem carbon and water fluxes during this severe drought event. Overall, we sought to better understand how the 2012-2015 California drought event affected ponderosa pines to inform future management practices in forests of the western United States.

ACKNOWLEDGMENTS

I would like to thank my advisor Steve Voelker for his support, guidance, and answers to my endless questions throughout this process. I would also like to thank my committee members, Barbara Bentz and Simon Wang, for providing their expertise to this project and for always having helpful advice when it was needed. Additionally, I would like to thank Sierra Oxborrow for her tireless assistance in the lab, and Jessika Pettit for being a sounding board for all of my ideas and frustrations.

I would also like to thank my family for their constant support and encouragement during this journey – especially my husband, Trevor Keen, who put in more than his fair share of hours proof-reading papers, listening to practice presentations, and reminding me to take a deep breath when things became stressful. Thank you for keeping me grounded.

Finally, I would like to thank our funding sources, the National Science Foundation (NSF) and the USDA Forest Service, and Utah State University for making this research possible.

Rachel Keen

CONTENTS

Page

LIST OF TABLES

LIST OF FIGURES

CHAPTER 1

INTRODUCTION

In recent decades, climate warming has had a significant impact on forest health in the western United States. Increasing temperatures and aridity have resulted in higher levels of drought stress and contributed to increased mortality across a broad range of forest types, fire regimes, tree species, and tree sizes (Allen et al. 2010). These changes are projected to continue and are expected to result in more severe and/or frequent large-scale mortality events (Allen et al. 2010). Changes in mortality rates, including massive dieback events like those seen in California over the past five years, can have serious effects on the ecological structure of a forest, impacting species composition and diversity as well as ecosystem functions that are economically important to our society (van Mantgem 2009; Adams et al. 2010; Anderegg et al. 2013).

Ponderosa pine (*Pinus ponderosa* Laws.) is one economically important species that is being impacted by increasing drought stress in the western United States (Waring and Law 2001). In addition to higher temperatures and increasing atmospheric and soil moisture stress, ponderosa pine is affected by subsequent increases in drought-related disturbances, including outbreaks of western pine beetle (*Dendroctonus brevicomis* Le Conte, Coleoptera: Scolytidae; WPB) and mountain pine beetle (*Dendroctonus ponderosae* Hopkins; MPB) (Bentz et al. 2010). Widespread tree mortality due to drought and bark beetle attacks has recently impacted many forests across the western United

States, but the relationship between drought stress and susceptibility to bark beetle attacks across tree species is not well understood.

Drought and climate in California

This study will focus on the 2012-2015 California drought event (hereafter referred to as the "CA Drought"); the severity of this multi-year drought is estimated to be a 1 in 1000 to 1 in ~10,000-year event (Griffin and Anchukaitis 2014; Robeson 2015). Although precipitation rates were very low during the CA Drought, levels were not outside the range of natural variability (Griffin and Anchukaitis 2014). However, in combination with record high temperatures, drought stress in California forests was severe. Multi-year drought events are common in central California, and are driven partially by ENSO, the El Niño-Southern Oscillation (Cayan et al. 1999). However, recent droughts and wet periods across California have not corresponded well with ENSO. The North American Winter Dipole, which has links to the Arctic Oscillation, has been shown to have significant influence on precipitation in California and much of the west coast since at least 1950 (Wang et al. 2015; Wang et al. 2017; Singh et al. 2019). The extreme drought conditions during the CA Drought were accompanied by a persistent, high-pressure ridge off the west coast of the United States and a low-pressure trough over the eastern United States. When the drought ended in the winter of 2016, this 'dipole' flipped—a low-pressure trough formed off the west coast and a high-pressure

ridge formed in the east—resulting in abnormally high precipitation rates and even severe flooding in California (Wang et al. 2017). Climate warming and increasing atmospheric greenhouse gas concentrations are expected to make these dipole events more frequent and severe in the future (Wang et al. 2015; Yoon et al. 2015), making it exceedingly important to understand how forests react to drastic inter-annual climatic variability and severe multi-year drought events.

Ponderosa pine and western pine beetle ecology

Ponderosa pine is a member of the Pinaceae family with an expansive range encompassing much of the western United States, spanning from southwestern Canada to Central Mexico (Shinneman et al. 2016; Willyard et al. 2017). Genetically distinct populations of ponderosa pine are associated with a variety of climate conditions throughout the central and western United States (Shinneman et al. 2016; Willyard et al. 2017) but two varieties are consistently recognized: *P. ponderosa* var. *ponderosa* Laws. (Pacific ponderosa pine) and *P. ponderosa* var. *scopulorum* Engelm. (Rocky Mountain ponderosa pine) (Potter et al. 2013; Shinneman et al. 2016; Willyard et al. 2017). The range of *P. ponderosa (*var. *ponderosa* Laws.) includes the southern Sierra Nevadas, CA, where this study takes place. Within *P. ponderosa* (var. *ponderosa* Laws), considerable genetic diversity associated with adaptations to differences in elevation and climate

conditions have been observed in the Sierra Nevada (Ager and Stettler 1983; Rehfeldt 1991; Weber and Sorensen 1992; Kolb et al. 2016; Warwell and Shaw 2018).

Ponderosa pine is one of many economically important timber species in the western United States (Oliver and Ryker 1990). Evolutionary traits of ponderosa pine, including thick protective bark, rapid growth of seedlings, and highly flammable litter, suggest adaptation to frequent low-intensity fires (Waring and Law 2001). These conditions were present in many regions of the western United States during the late Holocene and through the time of European settlement in the late 1800's (Guyette et al. 2012), but fire suppression efforts for the past century have nearly tripled the historic fire-return interval in many areas (Covington and Moore 1994; Steel et al. 2015). The absence of frequent low-intensity fire has allowed shade-tolerant and fire-intolerant species to establish and fill gaps in what were historically patchy or low-density forests dominated by fire-resistant species like ponderosa pine (Parsons and DeBenedetti 1979; Hood et al. 2016).

WPB is one of several bark beetle species that uses ponderosa pine as a host, but these beetles can also attack Coulter pines (*Pinus coulteri*), which inhabit the southern coastal mountains of California. WPB has a similar range to that of ponderosa pine, spanning much of western North America, and is typically found at elevations of 600-1800m (DeMars and Roettgering 1982). This species can produce multiple generations per year depending on how long, and how favorable, the growing season is. When populations are relatively low, WPB tends to attack damaged or severely stressed trees. Severity of outbreaks is typically higher in dense, even-aged stands and during years in

which more generations than normal are produced (i.e. warmer, longer growing season) (DeMars and Roettgering 1982). During an attack, female beetles attempt to enter the phloem of a tree by boring a hole through the bark. Ponderosa pines can defend against these attacks by producing flows of resin through the bore holes, essentially flushing the beetle out and preventing it from feeding on the phloem and colonizing the tree (DeMars and Roettgering 1982). Without sufficient defense resources, the tree may be unable to remove the beetle and become colonized. As the beetles enter the tree, they carry multiple fungal species that also infect the host tree (DeMars and Roettgering 1982). Warmer temperatures due to climate warming, particularly during the winter and spring, allow WPB to fly earlier in the year and possibly produce an additional generation during the growing season (Bentz et al. 2010; Anderegg et al. 2015).

Tree-ring growth and stable isotopes

Climate conditions during tree growth are recorded in annual growth rings and can be used to investigate tree physiological responses to drought and climate variability. For most low- to mid-elevation locations across the western United States and elsewhere, annual ring widths provide an estimate of growth that occurs each year, with less growth typically occurring during years in which trees are damaged or significantly stressed by drought or other factors (Fritts 1976). Tree-ring carbon and oxygen stable isotopes in tree ring cellulose can yield additional insights into climate conditions and physiological

responses of the trees in the past. Substantial work has been done using stable isotopes in ponderosa pine throughout its range in North America to look at climate patterns, annual precipitation, and intrinsic water-use efficiency (iWUE) (McDowell et al. 2003; Roden and Ehleringer 2007; Szejner et al. 2016; Voelker et al. 2019). Understanding how tree-ring measurements, including growth rates and stable isotopes, record and reflect climate conditions, ecosystem carbon and water fluxes, and physiological drought stress will improve our ability to predict forest responses to future climate conditions.

Objectives and motivations

In the first portion of this study (Chapter 2), the overarching goal was to better understand the relative roles of drought stress and forest density in tree mortality during the CA Drought and western pine beetle outbreak. Approximately 90% of mature ponderosa pines in the southern Sierra Nevadas died during this drought event (Fettig et al. 2019; Pile et al. 2019). In this study, trees that died during the drought were compared to nearby paired trees that survived to determine what physiological characteristics may have allowed for survival. Because projections of global climate change predict continually increasing temperatures as well as frequency and duration of drought conditions in the western United States (Asner et al. 2015), it is increasingly important to understand how forests will respond under these conditions. In the second portion of this study (Chapter 3), intra-annual tree-ring growth rates and stable carbon isotopes were

compared to ecosystem flux data during the CA Drought to determine the extent to which these tree-level measurements recorded ecosystem-scale carbon and water fluxes. This portion of the study also explored the ability to utilize tree-ring measurements as proxies for ecosystem-flux data. The ability to use tree-ring data in this way would be valuable in regions or localities where no flux towers exist (ex. steep terrain precludes the use of eddy covariance-based measurements of ecosystem gas fluxes), and/or when ecosystem flux data from the past could provide valuable context to modern flux tower measurements. This severe multi-year drought period and the availability of on-site flux data provide a unique opportunity to explore the relationship between tree- and ecosystem-scale carbon and water fluxes to better understand how trees respond to severe drought.

Understanding the physiological responses of trees to extreme drought, as well as the relationship between drought stress and bark beetle outbreak events, can give us more insight into how to manage at-risk forests, including how to increase resistance to future droughts and resilience to future disturbance, including bark beetle attacks and wildfires. Since many forests of the western United States contain economically important tree species, including ponderosa pine, landscape-scale mortality events can have disastrous consequences for local and regional economies for decades while forests recover. Additionally, these forests provide many valuable ecosystem functions, including habitat for other plants and animals, large-scale carbon storage, timber production, and recreation (Christensen et al. 2016). A better understanding of how trees respond to and record

severe drought events will allow us to better predict, and hopefully mitigate, future large-scale mortality events in the western United States.

References

Adams HD, Macalady AK, Breshears DD, Allen CD, Stephenson NL, Saleska SR, Huxman TE, McDowell NG (2010) Climate-induced tree mortality: earth system consequences. Eos, Transactions American Geophysical Union 91:153–154

Ager AA, Stettler RF (1982) Local variation in seeds of ponderosa pines. Canadian Journal of Botany 61:1337-1344

Allen CD, Macalady AK, Chenchouni H, Bachelet D, McDowell N, Vennetier M, Kitzberger T, Riglilng A, Breshears DD, Hogg EH, Gonzalez P, Fensham R, Zhang Z, Castro J, Demidova N, Lim JH, Allard G, Running SW, Semerci A, Cobb N (2010) A global overview of drought and heat-induced tree mortality reveals emerging climate change risks for forests. Forest Ecology and Management 259:660-684

Anderegg WL, Hicke JA, Fisher RA, Allen CD, Aukema J, Bentz BJ, Hood S, Lichstein JW, Macalady AK, McDowell N, Pan Y, Raff K, Sala A, Shaw JD, Stephenson NL, Tague C, Zeppel M (2015) Tree mortality from drought, insects, and their interactions in a changing climate. New Phytologist 208:674-683

Asner GP, Brodrich PG, Anderson CB, Vaughn N, Knapp DE, Martin RE (2017) Remote sensing of canopy water loss during the 2012-2015 California drought. PNAS E249-E255

Bentz BJ, Regniere J, Fettig CJ, Hansen M, Hayes JL, Hicke JA, Kelsey RG, Negron JF, Seybold SJ (2010) Climate change and bark beetles of the Western United States and Canada: Direct and indirect effects. Science 60:602-613

Cayan DR, Redmond KT, Riddle LG (1999) ENSO and hydrologic extremes in the western United States. Journal of Climate 12:2881-93

Christensen GA, Waddell KL, Stanton SM, Kuegler O (2016) California's forest resources: Forest Inventory and Analysis, 2001-2010. Gen. Tech. Rep. PNW-GTR-913. Department of Agriculture, Forest Service, Pacific Northwest Research Station, Portland, OR, USA

Covington WW, Moore MM (1994) Southwestern ponderosa forest structure. Changes since Euro-American settlement. Journal of Forestry 92:39–47

DeMars Jr. CJ, Roettgering BH (1982) Western pine beetle. Forest Insect and Disease Leaflet 1. US Department of Agriculture Forest Service, Washington DC, USA

Fettig, CJ, Mortenson, LA, Bulaon, BM, Foulk PB (2019) Tree mortality following drought in the central and southern Sierra Nevada, California, U.S. Forest Ecology and Management 432:164-178

Fritts HC (1976) Tree rings and climate. Academic Press, London, UK

Griffen D, Anchukaitis KJ (2014) How unusual is the 2012-2014 California drought? Geophysical Research Letters 41:9017-9023

Guyette RP, Stambaugh MC, Dey DC, Muzika RM (2012) Predicting fire frequency with chemistry and climate. Ecosystems 15:322-35

Hood SM, Baker S, Sala A (2016) Fortifying the forest: thinning and burning increase resistance to a bark beetle outbreak and promote forest resilience. Ecological Applications 0:1-17

Kolb TE, Grady KC, McEttrick MP, Herrero A (2016) Local-scale drought adaptation of ponderosa pine seedlings at habitat ecotones. Forest Science 62:641-651

McDowell N, Brooks JR, Fitzgerald SA, Bond BJ (2003) Carbon isotope discrimination and growth response of old Pinus ponderosa trees to stand density reductions. Plant, Cell & Environment 26:631-44

Oliver WW, Ryker RA (1990) Ponderosa pine. In: Burns RM, Honkala BH (eds) Silvics of North America: Conifers, vol. 1. Agricultural Handbook 654. USDA Forest Service, Washington, DC, USA, pp 413–424

Parsons DJ, DeBenedetti SH (1979) Impact of fire suppression on a mixed-conifer forest. Forest Ecology and Management 2:21-33

Pile LS, Meyer MD, Rojos R, Roe O, Smith MT (2019) Drought impacts and compounding mortality of forest trees in the southern Sierra Nevada. Forests 10 doi:10.3390/f10030237

Potter KM, Hipkins VD, Mahalovich MF, Means RE (2013) Mitochondrial DNA haplotype distribution patterns in Pinus ponderosa (Pinaceae): Range-wide evolutionary history and implications for conservation. American Journal of Botany 100:1562-79

Robeson SM (2015) Revisiting the recent California drought as an extreme value. Geophysical Research Letters 42:6771-6779

Roden JS, Ehleringer JR (2007) Summer precipitation influences the stable oxygen and carbon isotopic composition of tree-ring cellulose in Pinus ponderosa. Tree Physiology 27:491–501

Shinneman DJ, Means RE, Potter KM, Hipkins VD (2016) Exploring climate niches of ponderosa pine (*Pinus ponderosa* Douglas ex Lawson) haplotypes in the western United States: Implications for evolutionary history and conservation. PloS one 11(3):e0151811

Singh D, Ting M, Scaife AA, Martin N (2018) California winter precipitation predictability: Insights from the anomalous 2015–2016 and 2016–2017 seasons. Geophysical Research Letters 45:9972-80

Steel ZL, Stafford HD, Viers JH (2015) The fire frequency-severity relationship and the legacy of fire suppression in California forests. Ecosphere 6:1-23

Szejner P, Wright WE, Babst F, Belmecheri S, Trouet V, Leavitt SW, Ehleringer JR, Monson RK (2016) Latitudinal gradients in tree-ring stable carbon and oxygen isotopes reveal differential climate influences of the North American Monsoon

system. Journal of Geophysical Research: Biogeosciences doi:10.1002/2016JG003460

Van Mantgem PJ, Stephenson NL, Byrne JC, Daniels LD, Franklin JF, Fule PZ, Harmon ME, Larson AJ, Smith JM, Taylor AH, Veblen TT (2009) Widespread increase of tree mortality rates in the Western United States. Science 323:521-524

Voelker SL, Merschel AG, Meinzer FC, Ulrich DE, Spies TA, Still CJ (2019) Fire deficits have increased drought sensitivity in dry conifer forests: Fire frequency and tree-ring carbon isotope evidence from Central Oregon. Global change biology 25:1247-62

Wang S-Y, Huang W-R, Yoon J-H (2015) The North American winter 'dipole' and extremes activity: a CMIP5 assessment. Atmospheric Science Letters 16:338-345

Wang S-Y, Yoon J-H, Becker E, Gillies R (2017) California from drought to deluge. Nature Climate Change 7:465-468

Waring RH, Law BJ (2001) The ponderosa pine ecosystems and environmental stress: past, present and future. Tree Physiology 21:273-274

Warwell MV, Shaw RG (2018) Phenotypic selection on ponderosa pine seed and seedling traits in the field under three experimentally manipulated drought treatments. Evolutionary Applications 12:159–174

Weber JC, Sorensen FC (1992) Geographic variation in speed of germination in central Oregon ponderosa pine (*Pinus ponderosa* Dougl. ex Laws). Research Paper

PNW-RP-444. USDA Forest Service, Pacific Northwest Research Station, Portland, OR, USA

Willyard A, Gernandt DS, Potter K, Hipkins V, Marquardt P, Mahalovich MF, Langer SK, Telewski FW, Cooper B, Douglas C, Finch K (2017) Pinus ponderosa: A checkered past obscured four species. American Journal of Botany 104:161-81

Yoon J-H, Wang S-Y, Gillies RR, Kravitz B, Hipps L, Rasch PJ (2015) Increasing water cycle extremes in California and in relation to ENSO cycle under global warming. Nature Communications 6:8657

CHAPTER 2

STRONGER INFLUENCE OF GROWTH RATE THAN SEVERITY OF DROUGHT STRESS ON MORTALITY OF LARGE PONDEROSA PINES DURING THE 2012-2015 CALIFORNIA DROUGHT

Abstract

As the climate continues to warm, forests in the western United States and elsewhere are being subject to more frequent and severe drought events. The 2012-2015 California drought is a recent example where drought stress was exacerbated by an epidemic scale outbreak of western pine beetle (*Dendroctonus brevicomis*) and collectively resulted in widespread mortality of dominant canopy species like ponderosa pine (*Pinus ponderosa* Lawson & C. Lawson). Large-scale mortality events can have substantial and widespread effects on forest structure, species composition, and ecosystem function, but the physiological relationship between drought stress in ponderosa pine and susceptibility to western pine beetle attack is not well understood. In this study, we compare pairs of large surviving and beetle-killed ponderosa pines following the 2012-2015 California drought in the southern Sierra Nevadas (elevation 1160 m) to evaluate physiological characteristics related to survival. Inter-annual growth rates (basal area increment, BAI) and tree-ring stable isotopes ($\Delta^{13}C$ and $\delta^{18}O$) were utilized to compare severity of drought stress and climate sensitivity in ponderosa pines that survived and those that were killed by western pine beetle leading up to, and during,

the 2012-2015 drought event. Compared to trees that were killed, surviving trees had higher growth rates and grew in plots with lower conspecific basal area. However, there were no detectable differences in $\Delta^{13}C$, $\delta^{18}O$, or stable isotope sensitivity to drought-related meteorological variables between surviving and dead trees. These results indicate that differences in severity of drought stress had little influence on local, inter-tree differences in growth rate and survival of large ponderosa pines during the severe 2012-2015 California drought and associated western pine beetle outbreak. Although many previous studies have shown that large trees are generally more susceptible to drought and bark beetle attacks than small trees, our data suggest that large ponderosa pines were more resistant to drought stress and bark beetle attacks when they were in the upper echelon of growth rates among trees within a stand and across the landscape.

Introduction

Between 2010 and 2017, over 100 million trees died in California (CA) due to drought and bark beetle outbreaks. A large portion of this mortality (~96%) occurred during the 2012-2015 drought period (hereafter referred to as the "CA Drought") and these numbers were particularly severe for the central and southern portions of the Sierra Nevada, CA (Moore et al. 2017; Pile et al. 2019). A recent study quantifying mortality during this period found that ponderosa pine (*Pinus ponderosa* Lawson & C. Lawson), the dominant canopy tree species in many low- and mid-elevation forests in the Sierra

Nevada, experienced the highest rate of mortality relative to co-existing species like incense cedar (*Calocedrus decurrens*) (Fettig et al. 2019). At sites ranging from ~900-2200 m elevation in four national forests in the Sierra Nevada, ponderosa pine had an 89.6% mortality rate compared to only 23.2% for incense cedar. Mortality was especially severe at lower elevations (~1,100 m), with many sites experiencing 100% ponderosa pine mortality (Fettig et al. 2019). Large scale mortality of a dominant canopy tree species like ponderosa pine could have substantial and widespread effects on forest structure, species composition, biodiversity, and ecosystem function in California and across the western United States (van Mantgem 2009; Adams et al. 2010; Anderegg et al. 2015).

Increasing drought severity in the western United States is projected to continue and will likely result in more large-scale forest mortality events in the future, further threatening ecologically and economically important tree species like ponderosa pine (Allen et al. 2010). As the climate warms, ponderosa pines are also affected by increasing frequency and severity of disturbance, including outbreaks of western pine beetle (*Dendroctonus brevicomis*; WPB) (Kolb et al. 2016a) like the one seen during the CA Drought (Fettig et al. 2019). In California, WPB typically produces two and partial third generation per year depending on the length and temperature of the growing season (DeMars and Roettgering 1982). In other bark beetle species, higher winter temperatures can also result in less over-winter death (Bentz et al. 2010), and warm spring and summer temperatures can result in earlier WPB adult emergence, increasing the potential for a

successful third generation (Miller and Keen 1960). In these ways, climate warming can directly and positively influence WPB population sizes.

Climate warming may also indirectly affect WPB success by influencing ponderosa pine vigor and defensive capacity. Based on the growth-differentiation-balance hypothesis (Herms and Mattson 1992), drought severity can either increase plant defensive capabilities or reduce them (Kolb et al. 2016a). While mild or moderate drought stress may increase the allocation of carbon resources to defense, severe drought stress often results in stomatal closure and reduced photosynthesis, and/or failures in the phloem system, all of which can lead to carbon starvation and insufficient resources for defense (Kolb et al. 2016a; McDowell et al. 2011; Sevanto et al. 2014). Severe drought stress in trees is thought to increase susceptibility to bark beetle attacks (Raffa et al. 2008; Kolb et al. 2016). Aspects of stand structure and competition that can affect a tree's vigor and ability to mobilize carbon defenses are also known to impact survival during large beetle outbreaks (Waring and Pitmann 1985; Coops et al. 2009; Fettig et al. 2019). Nonetheless, the physiological relationship between drought stress in ponderosa pine and susceptibility to western pine beetle attack, particularly during severe drought events, is not well understood. A better understanding of these relationships could inform future management practices or provide more accurate predictions of forest mortality in a warmer and drier future.

Here we explore ponderosa pine physiological response to drought using tree ring widths and stable isotope analyses of tree-ring cellulose. Both have been used extensively to gain insight into past climate conditions and ponderosa pine response to climate

variability (McDowell et al. 2003; Roden and Ehleringer, 2007; Williams et al. 2010a; Leavitt et al. 2011; Williams et al. 2012; Szejner et al. 2016; Voelker et al. 2019). Tree-ring $\Delta^{13}C$ (biological discrimination against ^{13}C) is largely determined by the ratio of photosynthetic assimilation to stomatal conductance (Farquhar et al. 1989; McCarroll and Loader 2004; Ehleringer and Farquhar 1993). Thereby, tree-ring $\Delta^{13}C$ can be used to infer severity of drought stress for individual trees where leaf gas exchange is primarily limited by stomatal conductance, as in the dry summer conditions prevalent in the Mediterranean climate of central California. In an effort to avoid severe drought stress, stomatal conductance in ponderosa pines typically decreases as severity of drought conditions increases, resulting in greater use of ^{13}C and lower $\Delta^{13}C$ values (McDowell et al. 2003; Voelker et al. 2019). Tree-ring $\delta^{18}O$ can also be affected by stomatal conductance by way of the Peclet Effect (Barbour et al. 2004). When stomatal conductance is high, there is a larger flux of un-enriched xylem water into the leaf, resulting in lower $\delta^{18}O$ values recorded in tree-ring cellulose. When stomatal conductance decreases, this flux of un-enriched xylem water also decreases, resulting in higher $\delta^{18}O$ values recorded by photosynthetic signals transmitted to tree-ring cellulose (Edwards and Fritz 1986; Farquar and Lloyd 1993; Roden et al. 2000).

In this study, we employed annually resolved ring widths and stable isotope data from individual trees to seek a stronger understanding of physiological responses to drought stress in surviving versus recently WPB-killed ponderosa pines. The specific objectives of this study were to determine (1) what climate factors were most highly correlated with tree ring $\Delta^{13}C$ and $\delta^{18}O$, (2) whether stand density affected climate

sensitivity or growth rate in surviving or dead ponderosa pines, (3) whether surviving and dead trees differed in growth rates, and (4) whether dead trees exhibited signs of higher severity of drought stress than trees that survived, despite growing in the same climate conditions. Overall, this study sought to determine whether differences in ecophysiology over time could help explain the ability of certain ponderosa pines to survive severe drought conditions and a concurrent western pine beetle outbreak while a much larger proportion of ponderosa pines died in association with the CA Drought (Fettig et al. 2019; Pile et al. 2019).

Materials and methods

Study Area

Sampling for this project was conducted in the spring of 2017 at Soaproot Saddle, a Southern Sierra Critical Zone Observatory (SSCZO) site northeast of Fresno, CA (Figure 2-1). In this area, ponderosa pine-dominated mixed conifer forests occur between ~900 and 2,000 m elevation. Other common species in this region include incense cedar (*Calocedrus decurrens*), California black oak (*Quercus kelloggii*), sugar pine (*Pinus lambertiana*), Douglas fir (*Pseudotsuga menziesii*), and manzanita (Arctostaphylos spp.). Soaproot Saddle is located at 1,160 m elevation and receives ~800mm of precipitation each year. Mean minimum temperature in this region is 5.5°C and mean maximum temperature is 18°C (Goulden et al. 2012). A large portion of annual precipitation occurs

in the winter and spring, followed by a summer drought period. Historically, this ecosystem experienced frequent, low-intensity fires every 10-20 years that kept ponderosa pine-dominated forests “open and parklike” (Parsons and DeBenedetti 1979; North et al. 2005; Van de Water and Safford 2011; Hood et al. 2016). Since widespread fire suppression efforts have been in place over the past century, most of the forests in this region have transitioned to dense, mixed-conifer forests with higher populations of fire-intolerant and shade-tolerant understory species (Stephens et al. 2015). Sampling took place on 12 plots at Soaproot Saddle (Figure 2-1).

Field Data Collection

Pairs of surviving and dead ponderosa pines were selected based on their similar stature, estimated age, and proximity to one another; average distance between paired trees was ~75 m. Individuals selected as focus trees were estimated to be 100-150 years old. In order to more accurately compare the physiology of surviving versus dead trees, pairs were also chosen for similarity of growing conditions (i.e. slope, geomorphic position, and density of understory vegetation). Six pairs of surviving and dead trees were sampled (12 total focus trees) and three 12 mm-diameter increment cores were extracted from each focus tree at breast height (between 1.0 and 1.5 m from ground level).

A 15 m-radius fixed-area circular plot was established with each focus tree at the center (Figure 2-2). Information recorded for trees ≥ 20 cm DBH (diameter at breast height) within each plot included DBH, species, and status (surviving/dead, percent

needle retention, and evidence of WPB attack when applicable). Basal area was calculated for each fixed-area plot (15-m radius) using the following equation:

$$BA = \frac{\sum DBH^2 * 0.00007854}{Area} \quad (1)$$

Total basal area, including all species present in the plot, was calculated as well as basal area of ponderosa pine at each plot.

Additional increment cores from ponderosa pines sampled by Ferrell (2017) were also utilized in order to compare the focus trees in this study to a random sample of relatively old (100+ years) ponderosa pines that also grew at Soaproot Saddle. Locations of these randomly sampled trees relative to our focus trees are shown in Figure 2-1 and information regarding mean size and age of these trees can be found in table A-1.

Increment Core Preparation and Measurement

Each increment core was mounted on a wooden stave and sanded using increasingly higher-grit sand paper (120-400) to prepare cores for visual cross-dating and measurement of annual growth rings. Whole ring widths as well as separate early- and latewood widths were measured using MeasureJ2X software (Voortech Consulting). Visual cross-dating was then conducted to assign calendar years to the rings in each core (Stokes and Smiley 1968). Visual cross-dating between trees was confirmed using COFECHA, a statistical program that assesses cross-dating quality and accuracy (Holmes 1983). Ring width chronologies for each focus tree were detrended separately using a negative exponential spline first to remove the biological growth signal, then with a 100-

yr spline to isolate climate trends (Bunn 2008). All detrending was conducted in ARSTAN (Cook and Krusik 2014).

DBH and ring widths were used to calculate basal area increment (BAI) for focus trees and randomly sampled trees (Ferrell 2017) to determine annual growth rates. BAI was calculated from the outside-in, assuming circularity of the growing cambium and employed estimates of bark thickness (McDonald 1983; Larsen and Hann 1985) to adjust for differences in radial measurements inside and outside of the bark for each tree. To minimize the potential for bias in assessing growth rates for trees that differed among groups in DBH, the age-related trend in BAI for randomly sampled trees was calculated using equation (2) ($R^2 = 0.90$, $p < 0.01$; *data not shown*). Thereafter, BAI deviations (BAI_D) were calculated for each tree using equation (3).

$$Predicted\ BAI = 0.8751 * Age^{0.6304} \quad (2)$$

$$BAI_D = \frac{Observed\ BAI - Predicted\ BAI}{Predicted\ BAI} * 100 \quad (3)$$

Stable Isotope Analyses

For each core from the 12 focus trees, latewood for the years 1950-2016 was separated using a scalpel under a dissecting microscope. Cores from each individual tree were combined, then each latewood sample was ground to a fine powder and sealed in a mesh filter bag (mesh size 25 µm; ANKOM Technology, Macedon, NY). Samples were

bleached using sodium chlorite and glacial acetic acid to remove extractives from the wood, leaving only holocellulose (Leavitt and Danzer 1993). Next, sodium hydroxide and glacial acetic acid were used to remove hemicellulose and yield α-cellulose, which faithfully records the $\delta^{18}O$ signature recorded in the wood each year without exchanging with atmospheric water (Rinne et al. 2005). After isolating α -cellulose, each sample was homogenized in deionized water using an ultrasonic probe and subsequently freeze-dried (Laumer et al. 2009). Samples were then packed in tin ($\Delta^{13}C$) or silver ($\delta^{18}O$) capsules before being analyzed at the Center for Isotope Biogeochemistry (CSIB) at the University of California, Berkeley. The carbon isotope ratio of each sample was obtained using standard high temperature combustion in a vario-Pyrocube elemental analyzer interfaced with an IsoPrime/Elementar IsoPrime 100 gas phase isotope ratio mass spectrometer (IsoPrime Ltd., Manchester, UK). The oxygen isotope ratios were determined by pyrolyzing α-cellulose in an elemental analyzer (TC/EA, IsoPrime/Elementar vario-Pyrocube) and analyzing the resulting gas with an isotope ratio mass spectrometer (IsoPrime 100). The long-term precision does not exceed ± 0.1 *‰ for* $\delta^{13}C$ and 0.2 *‰* for $\delta^{18}O$ for the mass spectrometer employed at CSIB.

All $\delta^{13}C$ values were converted to carbon isotope discrimination values ($\Delta^{13}C$) following Farquhar et al. (1982):

$$\Delta^{13}C = \frac{\delta^{13}C_{air} - \delta^{13}C_{plant}}{1 + \delta^{13}C_{plant}/1000} \quad (4)$$

In this equation, $\delta\,^{13}C_{air}$ was estimated annually from the values given by McCarroll and Loader (2004) merged with more recent $\delta\,^{13}C_{air}$ records from Mauna Loa, Hawaii. $\Delta^{13}C$

and $\delta^{18}O$ isotope series that were intended for comparison to climate variability were detrended with ARSTAN software (Cook and Krusik 2014) using a 100-yr spline to isolate inter-annual to decadal climate trends from low-frequency variation that could arise due to changes in competition, tree height, or rooting depth. Residual isotope series were then multiplied by the mean isotopic value for each core to obtain a pre-whitened isotope series without autocorrelation for each focus tree. Due to poor cross-dating of isotope series with the other trees, two focus trees were removed from subsequent statistical analyses, resulting in a sample size of 10 focus trees.

Climate Data

The climate data employed were obtained through PRISM (http://prism.oregonstate.edu/) and ClimateWNA (http://www.climatewna.com/). Palmer Drought Severity Index (PDSI) data for California's 5th climate division was obtained through the National Oceanic and Atmospheric Association (NOAA). Climate variables, including PDSI, vapor pressure deficit (VPD), climatic moisture deficit (CMD), and precipitation were seasonally averaged for winter (previous December, current January and February), spring (March, April, May), summer (June, July, August), and fall (September, October, November). Seasonal climate data were pre-whitened to remove autocorrelation and long-term trends and to highlight inter-annual variation.

Statistical Analyses

Pre-whitened climate series were compared to similarly pre-whitened isotope chronologies for the years 1950-2016 and Pearson's correlation coefficients were calculated. Correlations were calculated separately for surviving and dead focus trees. 20-year moving window correlations were conducted for each climate variable with the $\Delta^{13}C$ record using the tidyquant package in R (Dancho and Vaughan 2018). Repeated measures mixed effects modeling using the package nlme (Pinheiro et al. 2016) in R was performed to determine whether significant isotopic differences ($\Delta^{13}C$ or $\delta^{18}O$) exist between surviving and dead trees. Focus tree pair (1-6) was included as the random variable with year, status (surviving or dead), and their interaction as predictors. A repeated measures mixed effects model was conducted for BAI_D with the same random and predictor variables to assess differences in growth rate. Trees sampled by Ferrell (2017) were included in this model. Similarly, a linear mixed effects model was used to compare basal area and percent dead ponderosa pine between plots with surviving and dead focus trees. Focus tree pair was included as a random variable and focus tree status (surviving or dead) as the predictor variable. Additionally, F-tests were used on pre-whitened isotope series to determine whether inter-annual variance in $\Delta^{13}C$ or $\delta^{18}O$ differed among surviving and dead focus trees.

Results

All dead focus trees had evidence of WPB attack, including pitch tubes, entrance holes, and gallery excavations, but we found no evidence of WPB attack on any of the surviving focus trees. This indicates that WPB attacks and subsequent effects of inoculation of trees with blue stain fungi (*Ceratocystis minor*) on xylem and phloem functionality were the proximate causes of mortality even though essentially all trees underwent moderate to severe drought stress. DBH was significantly greater in surviving trees than in dead trees ($p = 0.03$), but tree age was not significantly different between the two groups ($p = 0.20$).

Across the entire 1900-2016 period, ponderosa pines that survived the CA Drought and WPB outbreak had significantly higher BAI_D than trees that died ($p < 0.01$) (Figure 2-3). Although both groups of trees show a steep decline in growth rates during the drought, surviving trees displayed a slight uptick in growth during 2016 after this region received substantial rainfall during the previous winter. Other notable periods of low growth rates include severe multi-year droughts during 1987-1992 and 1929-1934, the latter being associated with the dust bowl droughts that affected much of North America (Jones 2015). Compared to tree core data collected at random locations across the same watershed by Ferrell (2017), both live and dead focus trees sampled in this study grew consistently faster since 1900. These randomly sampled trees also experienced a steep decline in growth during the CA Drought (Figure 2-3). The randomly

sampled trees had a mean DBH of 47.2 cm (±16 SD) and mean age of 115.3 years (±38 SD) (Table A-1).

Plot-scale basal area, calculated across all species, was compared between plots with a surviving focus tree and plots with a focus tree that was killed by WPB during the drought. There was no significant difference in total plot basal area between the two groups of plots when all tree species were included ($p = 0.55$). However, there was significantly greater ponderosa pine basal area at plots associated with a dead focus tree ($p = 0.01$). Additionally, there was significantly higher percent ponderosa pine mortality in plots with a dead focus tree ($p < 0.01$) (Figure 2-4). Plots with a dead focus tree had 100% mortality of ponderosa pines > 30 cm DBH.

Interestingly, there were no significant differences in latewood $\Delta^{13}C$ or latewood $\delta^{18}O$ between trees that survived and trees that were killed by WPB during the drought ($p = 0.99$ and $p = 0.16$, respectively) (Figure 2-5a-b). Dead focus tree $\Delta^{13}C$ showed elevated inter-annual variance compared to surviving focus trees (dead = 0.22 ‰; surviving = 0.17 ‰) but the difference was not significant ($p = 0.33$). Variance in dead focus tree $\delta^{18}O$ (1.52 ‰) was significantly higher than in surviving focus trees (0.65 ‰) ($p < 0.01$). When compared to spring and summer PDSI from 1950-2016, $\Delta^{13}C$ values were near their lower extreme during the CA Drought, particularly during 2014 which had the lowest PDSI and $\Delta^{13}C$ values for this time period (Figure 2-6).

For the years 1950-2016, Pearson's correlation coefficients were significant ($p < 0.05$) when greater than 0.24 or less than -0.24. Of the four climate variables tested (PDSI, VPD, CMD, and precipitation), only PDSI had significant correlations with $\delta^{18}O$,

and only with dead focus trees during the spring and summer (Table 2-2a). Overall, $\delta^{18}O$ was poorly correlated with drought-related climate variables during this time period. $\Delta^{13}C$ was positively correlated with PDSI and precipitation and negatively correlated with VPD and CMD. The highest correlations between $\Delta^{13}C$ and VPD, CMD, and precipitation were associated with the spring season, but $\Delta^{13}C$ was more closely related to PDSI during the summer season (Table 2-2b). This trend was consistent in both surviving and dead ponderosa pines. $\Delta^{13}C$ correlation strengths were similar for both groups of trees, although live focus trees had slightly stronger spring correlations for most climate variables.

To assess the stability of correlations between $\Delta^{13}C$ and drought-related climate variables, 20-year moving window correlations were calculated for the period 1900-2016. Because of the similarity in correlation strengths between $\Delta^{13}C$ and climate for surviving and dead focus trees (Table 2-2a), all data were combined for these analyses to provide the most accurate assessment of how the influence of climate may have changed over time for ponderosa pines in this area. These moving correlations revealed that the relationships between $\Delta^{13}C$ and spring season VPD, CMD, and precipitation have been increasing in strength since 1900 (Figure 2-7b-d). For PDSI, a similar increase in correlation occurs over time, but is associated with summer instead of spring conditions (Figure 2-6a), reflecting the same seasonal offset among climate variables observed in static correlations (Table 2-2a). The strength of this trend varies between climate variables but is strongest for the changing influence of spring precipitation ($r^2 = 0.74$).

Discussion

As the climate has continued to warm over the past several decades, the western United States has experienced increased aridity as well as more frequent and severe drought events (Allen et al. 2010). Warmer, drier conditions have resulted in longer growing seasons and earlier snowmelt in California (Gleick 1987; Stewart et al. 2004; Knowles and Cayan 2004; Mote et al. 2005). Moving correlation results from this study show that tree-ring $\Delta^{13}C$ correlations with spring drought-related climate variables (VPD, CMD, and precipitation) have been getting stronger since 1900 (Figure 2-7) (all seasons shown in figures A-1 through A-4), indicating an earlier onset of summer drought stress in these trees. Correlations with PDSI show this same trend, but during the summer. This offset is likely due to the considerable memory in soil moisture responses to climate, which is reflected in how PDSI is calculated (Mishra and Singh 2010). PDSI and $\Delta^{13}C$ values were both near their lower extremes during the CA Drought compared to the rest of the 1950-2016 period, particularly during 2014 (Figure 2-6), indicating severe drought stress in these ponderosa pines during the drought.

The primary difference between surviving and WPB-killed ponderosa pines found in this study was in growth rate. Relatively old and large trees that managed to survive the CA Drought and concurrent western pine beetle outbreak in this area were growing significantly faster than the trees that were killed (Figure 2-3). This difference in growth rate was observed across the entire 1900-2016 period, not just for a few decades prior to the drought. Given our paired sampling design that aimed to minimize plot-level

differences that could influence tree fitness, this result suggests that surviving trees were inherently different in some way than the trees that were killed by WPB during the drought.

The influence of growth rate on susceptibility to attack by a variety of bark beetle species is a common question, and results appear to vary based on elevation, climate conditions, and stand age (Cooper et al. 2018). The few studies that have specifically investigated how growth rates of ponderosa pine may influence attacks and/or mortality by WPB have shown that large, slower-growing trees are preferentially attacked under endemic beetle conditions, and at the beginning of an epidemic scale outbreak like the one seen during the CA Drought (Craighead 1925; Person 1928; Miller and Keen 1960). Mountain pine beetle (*Dendroctonus ponderosae*; MPB), another bark beetle species that attacks ponderosa pine in the western United States, has been studied more extensively, but the relationship between growth rate and mountain pine beetle attack success is still not clear. Multiple studies have shown that MPB preferentially attacks faster growing trees (Yanchuk et al. 2008; Margoles 2011; de la Mata et al. 2017) while others have shown the opposite trend (Waring and Pittman 1985; Coops et al. 2009; Knapp et al. 2013; Cooper et al. 2018).

A more extensive sampling of tree cores from this watershed was undertaken by Ferrell (2017) in 2015 before most trees had died. BAI data was calculated for a sub-set of these trees exceeding 100 years of age so that the results would be comparable to the trees sampled in this study. These randomly sampled trees had substantially lower BAI compared to both surviving and dead focus trees, despite being of similar age. Hence, our

dead focus trees exhibited growth rates that were faster than average for trees of a comparable age distribution, and our surviving trees grew faster yet than both of the previous groups. Since dead focus trees were growing in close proximity to surviving focus trees, it is clear that soil and stand conditions that promoted higher productivity also tended to favor the survival of faster growing trees on such plots. Therefore, the CA Drought and concurrent WPB outbreak was so severe across our study area that only the fastest of the fast-growing large, overstory ponderosa pines survived. Note that many more small ponderosa pines (i.e. < 30 cm DBH) survived compared to large ponderosa pines, but only in plots with a surviving focus tree (Fig. 2-4). However, this is likely not a consequence of tree size *per se*, but of the success of beetle brood production in trees with greater phloem thickness (Amman 1972; Graf et al. 2012), a trait which is strongly correlated with tree size as small trees tend to grow slower due to their subordinate status in closed canopy stands. Indeed, our findings from intensive growth and stable isotope measurements on a small number of trees are supported by more extensive forest inventory efforts that overlap with our Soaproot Saddle sampling location. Pile et al. (2019) also found that larger size in ponderosa pines was consistently associated with increased survival following the CA Drought and WPB outbreak.

During a less severe drought and/or bark beetle outbreak, it is possible that the growth rate threshold for survival would have been lower due to lower levels of drought stress and associated beetle pressure (Craighead 1925; Person 1928; Miller and Keen 1960). Although the randomly sampled trees (Ferrell 2017) were alive during sampling in 2015 and we do not have data on their post-drought status, ~50% of these trees had

missing rings in 2014 and 2015, suggesting that growth had slowed substantially or even stopped for half of all large ponderosa pines during the drought. Fettig et al. (2019) showed that ~89% of ponderosa pines (> 30 cm DBH) died during the drought. Therefore, it is likely that the majority of the trees that were alive and sampled randomly during the summer of 2015 died shortly thereafter. More light was shed on this particular sequence of mortality by Pile et al. (2019), who showed that the probability of a ponderosa pine surviving the drought through 2015 varied between ~60% to 90% depending on DBH, whereas the same trees sampled in 2017 varied in survival between ~10% to 30% depending on DBH.

There are several possible explanations for the faster growth rate observed in surviving large trees including 1) lower severity of drought stress relative to trees that were killed by WPB, 2) allocation of resources to aboveground growth at the expense of defense or belowground structures, or 3) earlier budbreak phenology resulting in a longer growing season. We expected to see evidence of more severe drought stress in trees that died compared to surviving trees. Among tree pairs, with comparable soil and plot conditions due to proximity, more severe drought stress likely would have resulted in slower growth and fewer resources for defense, making those trees more susceptible to western pine beetle attack. Additionally, previous studies comparing growth and tree-ring stable isotopes in surviving and dead trees determined that faster growing trees often exhibited lower water use efficiency (WUE), allowing them to grow quickly but risk hydraulic failure under drought conditions (reviewed in Gessler et al. 2018). As Gessler et al. (2018) notes, differences in water use efficiency would require differences in

stomatal conductance, which should show up in $\Delta^{13}C$ and $\delta^{18}O$ records where biologically and ecologically significant differences in leaf gas exchange exist.

In contrast with our predictions, we found no evidence of differences in absolute $\Delta^{13}C$ and $\delta^{18}O$ values or in the sensitivity to drought-related climate variables that may have suggested that stomatal constraints on leaf gas exchange differed between surviving and dead focus trees. According to theory underlying stable carbon isotopes (Farquhar et al. 1989; Dawson et al. 2002; McCarroll and Loader 2004), and stable oxygen isotopes (Edward and Fritz 1986; Farquhar and Lloyd 1993; Roden et al. 2000; Barbour et al. 2004), higher sensitivity to drought stress would have presented as lower $\Delta^{13}C$ values, higher $\delta^{18}O$ values, and stronger climate correlations in the dead focus trees relative to surviving focus trees. Instead, our results show that both groups of trees have had very similar $\Delta^{13}C$ and $\delta^{18}O$ records for the past ~65 years (Figure 2-5) and appear to be responding to climate in a similar way based on static correlations (Table 2-2). The lack of climate correlations with $\delta^{18}O$ is likely due to the fact that winter precipitation is typically the primary water source for many tree species, and increasingly so in dry habitats (Allen et al. 2019). This water-use strategy could result in a tree-ring $\delta^{18}O$ record that primarily reflects the values of winter precipitation $\delta^{18}O$ instead of evaporative enrichment during the growing season. As recent hydroclimatic variability in California has shown, dominant storm tracks can change greatly from year to year, and this can induce changes in precipitation $\delta^{18}O$ of individual storms on the order of 5 ‰ (Smith et al. 1979).

Due to the unprecedented severity of the CA Drought, it is likely that all ponderosa pines were stressed and therefore generally more susceptible to WPB attack (Raffa and Berryman 1983; Safranyik and Carrol 2006; Anderegg et al. 2015). If essentially all overstory trees – except for the fastest growing individuals on the most productive plots – were stressed past a certain threshold that allowed for successful WPB attack and population growth, it would explain why severity of drought stress among our large, relatively fast-growing focus trees did not influence survival.

Another possible explanation for the observed discrepancy in growth rates between surviving and dead focus trees is different growth-defense strategies. Higher allocation of resources to growth has been hypothesized to be associated with lower allocation of resources to defense and higher risk of mortality (Lorio 1986; Stamp 2003). However, McDowell et al. (2007) showed that BAI has a strong positive relationship with resin flow in ponderosa pine ($r^2 = 0.84$), which would suggest that faster growing ponderosa pines would have had greater capacity for defense against WPB attack compared to slower growing ponderosa pines. Similarly, Kane and Kolb (2010) found a positive relationship between BAI and resin duct production in ponderosa pines. The evidence we provide here, when combined with evidence from multiple previous studies showing that slower growing ponderosa pines are generally killed by bark beetles at a higher rate, supports a more general pattern whereby faster growing trees are more capable of defending themselves against attack. Although we did not directly measure defense traits, it is unlikely that faster growth in surviving ponderosa pines in this study was a result of lower allocation of resources to defense. However, at least one previous

study (Hood et al. 2015) found no relationship between ponderosa pine growth rates and resin duct production, indicating that growth rates may not always be a reliable measure of defensive capabilities (Bentz et al. 2016).

A third potential explanation for higher growth rates in surviving trees is earlier budbreak phenology that would have allowed some trees to take advantage of warming temperatures over the past 100+ years and gain more carbon earlier in the growing season before the onset of summer drought stress. In a large-scale review of plant resistance to herbivory by Carmona et al. (2011), plant susceptibility was better predicted by life history traits, including shoot elongation and budbreak, than by secondary metabolite production, including resin. Budbreak timing in ponderosa pines can differ by 20-40 days as a result of genetic differences between individuals, and a large-scale study by Rehfeldt (1991) showed that populations differing by only ~400 m can contain genetic differences in phenology that are influenced by length of the frost-free season and moisture stress. This distance is well within the range of pollen dispersal in open conifer forests (Di-Giovanni 1996; Williams 2010b; Eckert et al. 2015). Additional studies have shown this same influence of parent tree growing conditions on seedling productivity – in several studies, seedlings with parent trees from drier, lower elevation sites were more successful than others when grown or germinated under drought conditions (Ager and Stettler 1983; Weber and Sorensen 1992; Kolb et al. 2016b; Warwell and Shaw 2018). A common garden experiment conducted by Warwell and Shaw (2018) evaluated timing of ponderosa pine emergence and early development under drought conditions using seed sources from different elevations and climate conditions. Their results showed that

phenotypes with early emergence dates and high early-season shoot elongation were the most successful under drought conditions. Environmental benefits to early emergence include earlier access to limited resources and additional time for carbon fixation and growth before the onset of summer drought (Warwell and Shaw 2018).

A longer spring/early summer growing season would have been captured by early-budbreak trees during recent decades of warming and would have provided more time for leaf development and total photosynthetic carbon gain. In turn, this would lead to greater radial growth and sensitivity to spring climate conditions, both of which were observed in surviving trees in this study. In particular, surviving trees had greater earlywood BAI than trees that were killed by WPB ($p < 0.01$) and proportionally greater earlywood BAI compared to latewood BAI, indicating that more growth was produced in the spring and early summer. It is therefore possible that surviving trees in our study were pollinated by sources at lower elevations or coastal regions (i.e. from trees locally adapted to historically warmer climate conditions), resulting in earlier phenology, longer growing seasons, and more growth production in the spring and early summer. Overall, we suggest that more attention should be paid to investigating how the affects of population genetics on phenology may impact drought survival of conifers in a warming world.

In addition to having faster growth rates, surviving trees in this study also grew in plots that contained significantly less ponderosa pine basal area compared to plots with a dead focus tree ($p = 0.01$). Again, wider forest inventory efforts support our findings that the probability of survival for ponderosa pines was weakly tied to the amount of

ponderosa pine at a given plot in 2015, and strongly related in 2017 (Pile et al. 2019). In contrast, Pile et al. (2019) showed that ponderosa pine survival was bolstered by higher overall forest basal area. Together, their results suggest that total competition was not a strong factor in mortality of ponderosa pine, but that host availability and/or the degree of local clustering of conspecifics did impact survival during, and following, CA Drought and WPB outbreak. Broadly speaking, availability of susceptible host trees has been shown to affect the likelihood of bark beetle infestation and mortality in numerous studies (McCambridge et al. 1982; Olsen et al. 1996; Negron and Popp 2004; Fettig et al. 2007). Although greater density of host trees in a plot would influence the likelihood of the focus tree being attacked by WPB, growth rates were not influenced by total basal area of all species in a plot. Regression analyses showed no significant relationship between surviving or dead average BAI with total plot basal area (surviving, $p = 0.65$; dead, $p = 0.66$) or ponderosa pine basal area (surviving, $p = 0.64$; dead, $p = 0.98$). These results, along with $\Delta^{13}C$ and $\delta^{18}O$ isotope records and climate correlations, suggest that severity of summer drought stress had little influence on local, inter-tree differences in growth rate and survival of large ponderosa pines during the CA Drought and WPB outbreak.

Conclusion

In this study, located near the epicenter of drought severity during the CA Drought, we compared inter-annual variation in growth rates and tree-ring $\Delta^{13}C$ and $\delta^{18}O$ between ponderosa pines that survived and those that were killed by WPB. We did not find evidence for differences in severity of drought stress between surviving and dead trees for ~65 years preceding the drought, indicating that other factors had a stronger influence on tree survival. Surviving trees had higher growth rates and grew in plots with lower ponderosa pine basal area than trees that were killed by WPB, and these findings are supported by wider forest monitoring efforts in the southern Sierra Nevadas (Pile et al. 2019). Our results support the explanation that ponderosa pine survival was driven by 1) greater growth rates, potentially due to earlier phenology that provided relatively greater carbon resources during a period of climate warming, and 2) relative isolation from conspecific host species that could provide some buffer from intensity of beetle attacks. Although the benefits of isolation to the likelihood of conifer survival during bark beetle outbreaks are well understood, the hypothesis that an earlier phenology may promote greater fitness in the face of combined pressures by drought and bark beetles deserves more in-depth testing across other regions and additional tree and bark beetle species.

References

Adams HD, Macalady AK, Breshears DD, Allen CD, Stephenson NL, Saleska SR, Huxman TE, McDowell NG (2010) Climate-induced tree-mortality: Earth system consequences. Eos, Transactions American Geophysical Union 91:153–154

Ager AA, Stettler RF (1983) Local variation in seeds of ponderosa pines. Canadian Journal of Botany 61:1337-1344

Allen CD, Macalady AK, Chenchouni H, Bachelet D, McDowell N, Vennetier M, Kitzberger T, Riglilng A, Breshears DD, Hogg EH, Gonzalez P, Fensham R, Zhang Z, Castro J, Demidova N, Lim JH, Allard G, Running SW, Semerci A, Cobb N (2010) A global overview of drought and heat-induced tree mortality reveals emerging climate change risks for forests. Forest Ecology and Management 259:660-684

Amman GD (1972) Mountain pine beetle brood production in relation to thickness of lodgepole pine phloem. Journal of Economic Entomology 65:138-140

Anderegg WL, Hicke JA, Fisher RA, Allen CD, Aukema J, Bentz BJ, Hood S, Lichstein JW, Macalady AK, McDowell N, Pan Y, Raffa K, Sala A, Shaw JD, Stephenson NL, Tague C, Zeppel M (2015) Tree mortality from drought, insects, and their interactions in a changing climate. New Phytologist 208:674-683

Barbour MM, Roden JS, Farquhar GD, Ehleringer JR (2004) Expressing leaf water and cellulose oxygen isotope ratios as enrichment above source water reveals evidence of a Peclet effect. Oecologia 138:426-435

Bentz BJ, Regniere J, Fettig CJ, Hansen M, Hayes JL, Hicke JA, Kelsey RG, Negron JF, Seybold SJ (2010) Climate change and bark beetles of the Western United States and Canada: Direct and indirect Effects. Science 60:602-613

Bentz BJ, Hood SM, Hansen EM, Vandygriff JC, Mock KE (2017) Defense traits in the long-lived Great Basin bristlecone pine and resistance to the native herbivore mountain pine beetle. New Phytologist 213:611-24

Bunn AG (2008) A dendrochronology program library in R (dplR). Dendrochronologia 26(2):115-124

Carmona D, Lajeunesse MJ, Johnson MJ (2011) Plant traits that predict resistance to herbivores. Functional Ecology 25:358-367

Cook ER, Krusic PJ (2014) ARSTAN version 44h3: A tree-ring standardization program based on detrending and autoregressive time series modeling, with interactive graphics. Tree-Ring Laboratory, Lamont-Doherty Earth Observatory of Columbia University, Palisades, New York, USA

Cooper LA, Reed CC, Ballantyne AP (2018) Mountain pine beetle attack faster growing lodgepole pine at low elevations in western Montana, USA. Forest Ecology and Management 427:200-207

Coops NC, Waring RH, Wulder MA, White JC (2009) Prediction and assessment of bark beetle-induced mortality of lodgepole pine using estimates of stand vigor derived from remotely sensed data. Remote Sensing and Environment 113:1058-1066

Craighead, FC (1925) The dendroctonus problem. Journal of Forestry 23:340-354

Dancho M, Vaughan D (2018) Tidyquant: Tidy quantitative financial analysis. URL: https://bit.ly/2KuBP98

Dawson TE, Mambelli S, Plamboeck AH, Templer PH, Tu KP (2002) Stable isotopes in plant ecology. Annual review of ecology and systematics 33:507-59

De la Mata R, Hood S, Sala A (2017) Insect outbreak shifts the direction of selection from fast to slow growth rates in the long-lived conifer *Pinus ponderosa*. Proceedings of the National Academy of Sciences 114:7391-7396

DeMars Jr. C.J, Roettgering BH (1982) Western pine beetle. Forest insect and disease Leaflet 1. USDA Forest Service, Washington DC, USA

DiGiovanni F, Kevan P, Arnold J (1996) Lower planetary boundary layer profiles of atmospheric conifer pollen above a seed orchard in northern Ontario, Canada. Forest Ecology and Management 83:87–97

Eckert, AJ, Maloney, PE, Vogler, DR, Jensen, CE, Mix, AD, Neale, DB (2015) Local adaptation at fine spatial scales: an example from sugar pine (*Pinus lambertiana*, Pinaceae). Tree Genetics & Genomes 11:1-17

Edwards TWD, Fritz P (1986) Assessing meteoric water composition and relative humidity from 18O and 2H in wood cellulose: Paleoclimatic implications for southern Ontario. Can. J. Earth Sci. 22:1720–1726

Ehleringer JR, Hall AE, Farquhar GD (eds) (1993) Stable Isotopes and Plant Carbon–Water Relations. Academic Press, New York

Farquhar GD, Lloyd J (1993) Carbon and oxygen isotope effects in the exchange of carbon dioxide between terrestrial plants and the atmosphere. In: Ehleringer JR, Hall AE, Farquhar GD (eds) Stable Isotopes and Plant Carbon–Water Relations. Academic Press, San Diego, CA, pp 47–70

Farquhar GD, Ehleringer JR, Hubick KT (1989) Carbon isotope discrimination and photosynthesis. Annu. Rev. Plant Physiol. Plant Mol. Biol. 40:503-537

Ferrell, RM (2017) *Patterns of above-ground ecosystem interactions of regolith in the southern Sierra Nevada of California* (Unpublished master's thesis). University of California, Davis, CA

Fettig, CJ, Klepzig, KD, Billings, RF, Munson, AS, Nebeker, EN, Negron, JF, Nowak JT (2007) The effectiveness of management practices for prevention and control of bark beetle infestations in coniferous forests of the western and southern United States. Forest Ecology and Management 238:24-53

Fettig, CJ, Mortenson, LA, Bulaon, BM, Foulk PB (2019) Tree mortality following drought in the central and southern Sierra Nevada, California, U.S. Forest Ecology and Management 432:164-178

Gessler A, Cailleret M, Joseph J, Schönbeck L, Schaub M, Lehmann M, Treydte K, Rigling A, Timofeeva G, Saurer M (2018) Drought induced tree mortality-a tree-ring isotope based conceptual model to assess mechanisms and predispositions. The New Phytologist 219:485

Gleick PH (1987) Regional hydrologic consequences of increases in atmospheric CO_2 and other trace gases. Climatic Change 10:137-60

Goulden ML, Anderson RG, Bales RC, Kelly AE, Meadows M, Winston GC (2012) Evapotranspiration along an elevation gradient in the Sierra Nevada. Journal of Geophysical Research 117 DOI:10.1029/2012JG002027

Graf M, Reid ML, Aukema BH, Lindgren BS (2012) Association of tree diameter with body size and lipid content of mountain pine beetles. The Canadian Entomologist 144:467-477

Herms DA, Mattson WJ (1992) The dilemma of plants: to grow or defend. Quarterly Review of Biology 67:282–335

Holmes RL (1983) Computer-assisted quality control in tree-ring dating and measurement. Tree Ring Bull. 43:69-78

Hood S, Sala A (2015) Ponderosa pine resin defenses and growth: metrics matter. Tree Physiology 35:1223-35

Hood SM, Baker S, Sala A (2016) Fortifying the forest: thinning and burning increase resistance to a bark beetle outbreak and promote forest resilience. Ecological Applications 0:1-17

Jones J (2015) California's most significant droughts: comparing historical and recent conditions. California Department of Water Resources, Sacramento, CA

Kane JM, Kolb TE (2010) Importance of resin ducts in reducing ponderosa pine mortality from bark beetle attack. Physiological Ecology 161:601-609

Knapp PA, Soule PT, Maxwell JT (2013) Mountain pine beetle selectivity in old-growth ponderosa pine forests, Montana, USA. Ecology and Evolution 3:1141-1148

Kolb TE, Fettig CJ, Ayres MP, Bentz BJ, Hicke JA, Mathiasen R, Steward JE, Weed AS (2016a) Observed and anticipated impacts of drought on forest insects and diseases in the United States. Forest Ecology and Management 380:321-334

Kolb TE, Grady KC, McEttrick MP, Herrero A (2016b) Local-scale drought adaptation of ponderosa pine seedlings at habitat ecotones. Forest Science 62(6): 641-651

Larsen DR, Hann DW (1985) Equations for predicting diameter and squared diameter inside bark at breast height for six major conifers of southwest Oregon. Research Note 77. Forest Research Laboratory, Corvallis, OR, USA

Laumer W, Andreu L, Helle G, Schleser GH, Wieloch T, Wissel, H (2009) A novel approach for the homogenization of cellulose to use micro-amounts for stable isotope analysis. Rapid Commun. Mass Spectrom. 23:1934-1940

Leavitt SW, Danzer SR (1993) Method for batch processing small wood samples to holocellulose for stable isotope analysis. Anal. Chem. 65:87-89

Leavitt SW, Woodhouse CA, Castro CL, Wright WE, Meko DM, Touchan R, Griffin D, Ciancarelli B (2011) The North American monsoon in the US Southwest: Potential for investigation with tree-ring carbon isotopes. Quaternary International 235:101–107

Lorio, PL (1986) Growth-differentiation balance: A basis for understanding southern pine beetle-tree interactions. Forest Ecology and Management 14:259-273

Margoles DS (2011) *Mountain pine beetle-Whitebark pine dynamics in a subalpine ecosystem of the Pioneer mountains, southwest Montana* (Unpublished master's thesis). University of Minnesota, Minneapolis, MN, USA

McCambridge WF, Hawksworth FG, Edminster CB, Laut JG (1982) Ponderosa pine mortality resulting from a mountain pine beetle outbreak. Research Paper RMRP-235. USDA Forest Service, Fort Collins, CO, USA

McCarroll D, Loader NJ (2004) Stable isotopes in tree rings. Quaternary Science Reviews 23:771-801

McDonald PM (1983) Local volume tables for Pacific madrone, tanoak, and California black oak in north-central California. Research Note PSW-362. USDA Forest Service, Pacific Southwest Forest and Range Experiment Station, Berkeley, CA, USA

McDowell M, Brooks JR, Fitzgerald SA, Bond BA (2003) Carbon isotope discrimination and growth response of old Pinus ponderosa trees to stand density reductions. Plant, Cell and Environment 226:631-644

McDowell, NG, Adams, HD, Bailey, JD, Kolb TE (2007) The role of stand density on growth efficiency, leaf area index, and resin flow in southwestern ponderosa pine forests. Canadian Journal of Forestry Research 37:343-355

McDowell NG, Beerling DJ, Breshears DD, Fisher RA, Raffa KF, Stitt M (2011) The interdependence of mechanisms underlying climate-driven vegetation mortality. Trends in Ecology and Evolution 26:523–532

Miller JM, Keen FP (1960) Biology and control of the western pine beetle: A summary of the first fifty years of research. USDA, Washington DC, USA

Mishra AK, Singh VP (2010) A review of drought concepts. Journal of Hydrology. 391:202-216

Moore J, McAfee L, Jirka A, Heath Z, Smith B (2017) 2016 Aerial Survey Results California. Research Paper R5-Pr-034. USDA Forest Service, Pacific Southwest Region, USA

Mote PW, Hamlet AF, Clark MP, Lettenmaier DP (2005) Declining mountain snowpack in western North America. Bulletin of the American meteorological Society 86:39-50

Negrón JF, Popp JB (2004) Probability of ponderosa pine infestation by mountain pine beetle in the Colorado Front Range. Forest Ecology and Management. 191:17–27

North M, Hurteau M, Fiegener R, Barbour M (2005) Influence of fire and El Nino on tree recruitment by species in Sierran mixed conifer. Forest Science 51:187-197

Olsen WK, Schmid JM, Mata SA (1996) Stand Characteristics Associated with Mountain Pine Beetle Infestations in Ponderosa Pine. Forest Science 42:310-327

Parsons DJ, DeBenedetti SH (1979) Impact of fire suppression on a mixed-conifer forest. Forest Ecology and Management 2:21-33

Person HL (1928) Tree selection by the western pine beetle. Jour. Forestry 26: 564-578

Pile LS, Meyer MD, Rojos R, Roe O, Smith MT (2019) Drought impacts and compounding mortality of forest trees in the southern Sierra Nevada. Forests 10 doi:10.3390/f10030237

Pinheiro J, Bates D, R Core Team (2015). nlme: Linear and Nonlinear Mixed Effects Models. R package version 3.1-121. URL: http://CRAN.R-project.org/package=nlme

Raffa KF, Berryman AA (1983) The role of host plant resistance in the colonization behavior and ecology of bark beetles (Coleoptera: Scolytidae). Ecological Monographs 53:27–49

Raffa KF, Aukema BH, Bentz BJ, Carroll AL, Hicke JA, Turner MG, Romme WH (2008) Cross-scale drivers of natural disturbances prone to anthropogenic amplification: the dynamics of bark beetle eruptions. BioScience 58:501-517

Rehfeldt, GE (1991) A model of genetic variation for *Pinus ponderosa* in the Inland Northwest (USA): applications in gene resource management. Canadian Journal of Forestry Research 21:1491-1500

Rinne KT, Boettger T, Loader NJ, Robertson I, Switsure VR, Waterhouse JS (2005) On the purification of a-cellulose from resinous wood for stable isotope (H, C and O) analysis. Chemical Geology 222:75-82

Roden JS, Lin G. Ehleringer JR (2000a) A mechanistic model for interpretation of hydrogen and oxygen isotope ratios in tree-ring cellulose. Geochemica et Cosmochimica Acta 64:21-35

Roden JS, Ehleringer JR (2007) Summer precipitation influences the stable oxygen and carbon isotopic composition of tree-ring cellulose in Pinus ponderosa. Tree Physiology 27:491–501

Safranyik L, Carroll AL (2006) The biology and epidemiology of the mountain pine beetle in lodgepole pine forests. In: Safranyik L, Wilson B (eds) The Mountain Pine Beetle: A Synthesis of Its Biology, Management and Impacts on Lodgepole Pine. Canadian Forest Service, Pacific Forestry Centre, Natural Resources Canada, pp 3-66

Sevanto S, McDowell NG, Dickman LT, Pangle R, Pockman WT (2014) How do trees die? A test of the hydraulic failure and carbon starvation hypothesis. Plant, Cell & Environment 37:153-161

Smith GI, Friedman I, Klieforth H, Hardcastle K (1979) Areal distribution of deuterium in eastern California precipitation, 1968-1969. Journal of Applied Meteorology 18:172-188

Stamp, N (2003) Out of the quagmire of plant defense hypothesis. The Quarterly Review of Biology 78:23-55

Stephens SL, Lydersen JM, Collins BM, Fry DL, Meyer MD (2015) Historical and current landscape-scale ponderosa pine and mixed conifer forest structure in the Southern Sierra Nevada. Ecosphere 6:1-63

Stewart IT, Cayan DR, Dettinger MD (2004) Changes in snowmelt runoff timing in western North America under a business as usual climate change scenario. Climatic Change 62:217-32

Stokes MA, Smiley T (1968) An Introduction to Tree-Ring Dating. University of Chicago Press, Chicago

Szejner P, Wright WE, Babst F, Belmecheri S, Trouet V, Leavitt SW, Ehleringer JR, Monson RK (2016) Latitudinal gradients in tree-ring stable carbon and oxygen isotopes reveal differential climate influences of the North American Monsoon system. Journal of Geophysical Research: Biogeosciences doi:10.1002/2016JG003460.

Van de Water KM, Safford HD (2011) A summary of fire frequency estimates for California vegetation before Euro-American settlement. Fire Ecology 7:26-58

Van Mantgem PJ, Stephenson NL, Byrne JC, Daniels LD, Franklin JF, Fule PZ, Harmon ME, Larson AJ, Smith JM, Taylor AH, Veblen TT (2009) Widespread increase of tree mortality rates in the Western United States. Science 323:521-524

Voelker SL, Merschel AG, Meinzer FC, Ulrich DEM, Spies TA, Still CJ (2019) Fire deficits have increased drought-sensitivity in dry conifer forests; fire frequency and tree-ring carbon isotope evidence from Central Oregon. Global Change Biology https://doi.org/10.1111/gcb.14543

Waring RH, Pitman GB (1985) Modifying lodgepole pine stands to change susceptibility to mountain pine beetle attack. Ecology 66:889-97

Warwell MV, Shaw RG (2018) Phenotypic selection on ponderosa pine seed and seedling traits in the field under three experimentally manipulated drought treatments. Evolutionary Applications 12:159–174

Weber JC, Sorensen FC (1992) Geographic variation in speed of germination in central Oregon ponderosa pine (*Pinus ponderosa* Dougl. ex Laws). Research Paper PNW-RP-444. USDA Forest Service, Pacific Northwest Research Station, Portland, OR, USA

Williams AP, Allen CD, Millar CI, Swetnam TW, Michaelsen J, Still CJ, Leavitt SW (2010a) Forest responses to increasing aridity and warmth in the southwestern United States. PNAS USA 107: 21298-21294

Williams, CG (2010b) Long-distance pine pollen still germinates after meso-scale dispersal. American Journal of Botany 97:846-855

Williams AP, Allen CD, Macalady AK, Griffin D, Woodhouse CA, Meko DM, Swetnam TW, Rauscher SA, Seager R, Grissino-Mayer HD, Dean JS, Cook ER, Gangodagamage C, Cai M McDowell NG (2012) Temperature as a potent driver of regional forest drought stress and tree mortality. Nature Climate Change 3:292-297

Yanchuk AD, Murphy JF, Wallin KF (2008) Evaluation of genetic variation of attack and resistance in lodgepole pine in the early stages of a mountain pine beetle outbreak. Tree Genetics and Genomes 4:171-180

Tables and Figures

Table 2-1 Status, DBH, height, and age of the focus tree at each plot, grouped by pair. Additionally, number of trees, total basal area (Total BA) with all species included, basal area of ponderosa pine only (PIPO BA), and percent dead ponderosa pine basal area (% Dead PIPO) at each plot.

Tree Pair	Status	DBH (cm)	Height (m)	Age	# of Trees	Total BAI (m^2 / ha)	PIPO BA (m^2 / ha)	% Dead PIPO BA
1	**Live**	93	40	187	11	34.17	14.32	53.9
	Dead	63	36.5	150	8	22.55	19.69	87.3
2	**Live**	74.9	39.2	119	23	42.39	16.34	11.3
	Dead	62.5	36.7	119	17	26.71	20.91	96.7
3	**Live**	119.5	42.7	247	15	28.49	9.47	48.3
	Dead	95.2	42.8	167	35	52.17	39.17	91.0
4	**Live**	77.7	31.7	178	15	22.85	15.66	46.3
	Dead	64.1	35.1	174	18	38.12	23.74	74.0
5	**Live**	100	43	133	20	37.6	29.97	41.6
	Dead	62.9	48	101	22	41.8	36.11	86.4
6	**Live**	96.6	34.5	169	12	24.21	8.62	7.4
	Dead	112.8	55.5	201	21	28.96	14.86	70.5

Table 2-2 Pearson's correlation coefficients for $\Delta^{13}C$ (A) and $\delta^{18}O$ (B) records compared to multiple climate variables. Data used for correlations include pre-whitened isotope data and residual climate data (detrended to remove long-term directional trends). Monthly climate data was averaged by season (Winter – DJF, Spring – MAM, Summer – JJA, Fall – SON) and compared to long-term isotope data for the same years (1950-2016). Significant correlations with p-values < 0.05 (≥ 0.24 or ≤ -0.24) and are denoted by (**). Correlations with p-values < 0.1 (≥ 0.20 or ≤ -0.20) are denoted by (•). P-vales for all correlations are shown in Table A-2).

A) $\Delta^{13}C$

	Surviving Focus Trees				*Dead Focus Trees*			
	Winter	**Spring**	**Summer**	**Fall**	**Winter**	**Spring**	**Summer**	**Fall**
PDSI	**0.49****	**0.68****	**0.73****	**0.58****	**0.56** **	**0.68****	**0.73****	**0.61****
VPD	-0.19	**-0.68****	**-0.41****	-0.15	**-0.33****	**-0.52****	**-0.46****	-0.18
CMD	-0.03	**-0.65****	**-0.35****	**-0.21**$^{\bullet}$	-0.15	**-0.49****	**-0.44****	-0.1
Precip	**0.26****	**0.59****	**0.21**$^{\bullet}$	0.04	**0.4****	**0.52****	**0.28****	-0.04

B) $\delta^{18}O$

	Winter	**Spring**	**Summer**	**Fall**	**Winter**	**Spring**	**Summer**	**Fall**
PDSI	0.02	0.01	0.03	-0.12	**0.21**$^{\bullet}$	**0.27****	**0.32****	0.19
VPD	-0.07	0.04	-0.09	0.06	-0.13	-0.17	0.04	0.09
CMD	**-0.22**$^{\bullet}$	0.04	-0.05	0.15	-0.14	-0.14	0.05	**0.22**$^{\bullet}$
Precip	-0.07	-0.07	-0.02	-0.08	0.02	0.16	-0.05	**-0.21**$^{\bullet}$

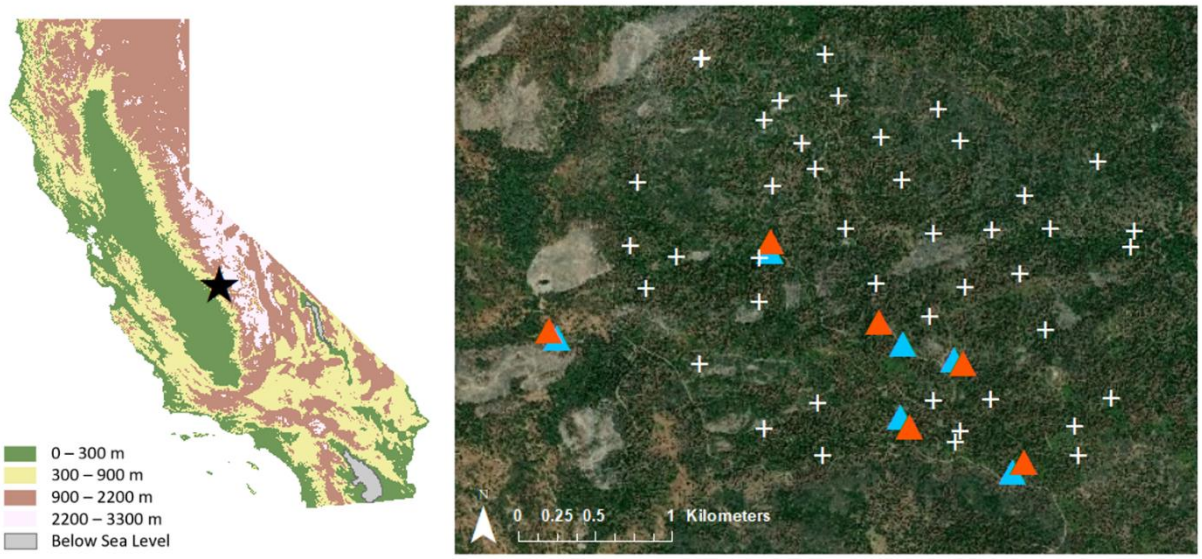

Fig. 2-1 Location of the Soaproot Saddle field site (black star) in central California (37.03N, 119.25W) (left panel). Plot locations at Soaproot Saddle (right panel). Blue triangles represent plots with surviving focus trees, red triangles represent plots with dead focus trees. Surviving and dead focus tree plots in close proximity are paired trees. White crosses represent trees randomly sampled in 2015 by Ferrell (2017).

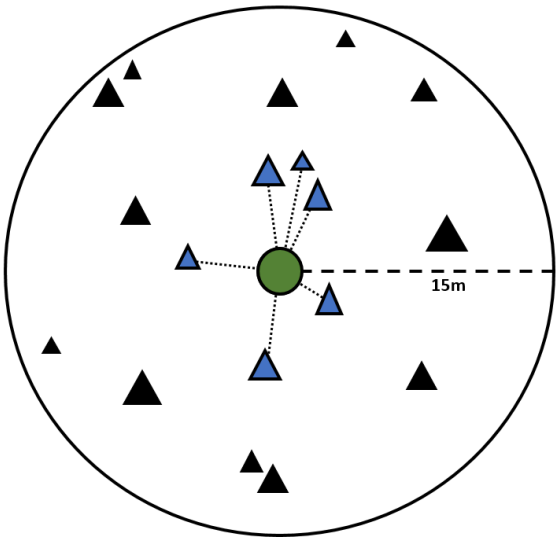

Fig. 2-2 Example of the fixed-area plot design for this study. Green filled circle represents the focus ponderosa pine and plot center. A 15m-radius fixed-area plot was established around each focus tree. Triangles represent trees in the plot with DBH ≥ 20cm, and blue filled triangles represent the six trees closest to the focus tree. Distance to focus tree (small dashed lines) and height were measured for these six trees at each plot.

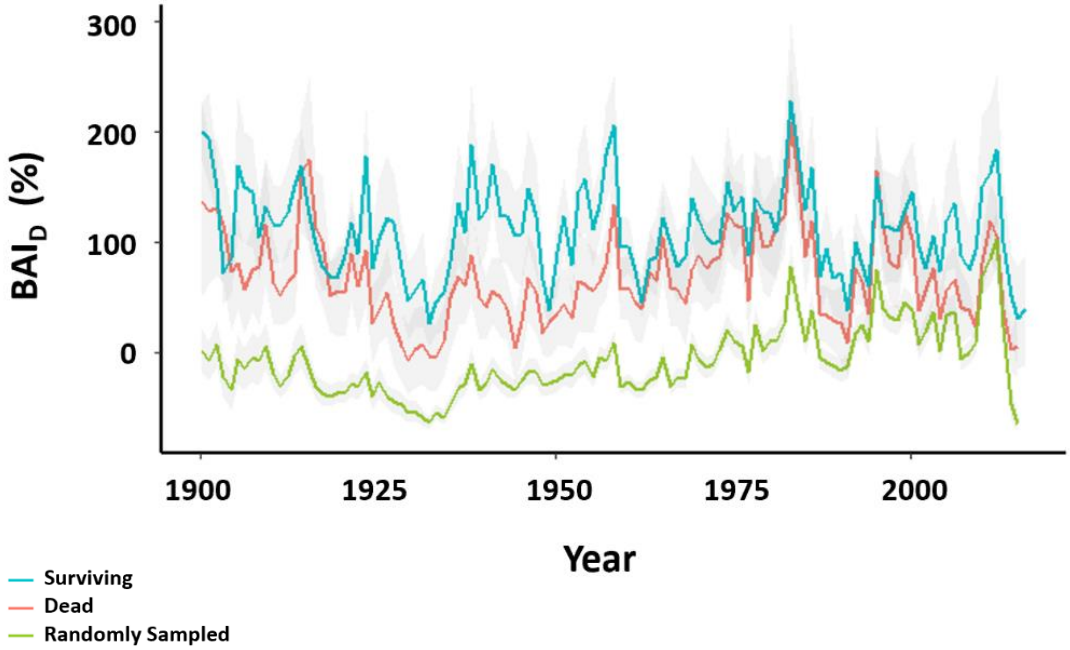

Fig. 2-3 BAI deviations (BAI_D) (%) for surviving (blue), dead (red), and randomly sampled (green) ponderosa pines from 1900-2016.

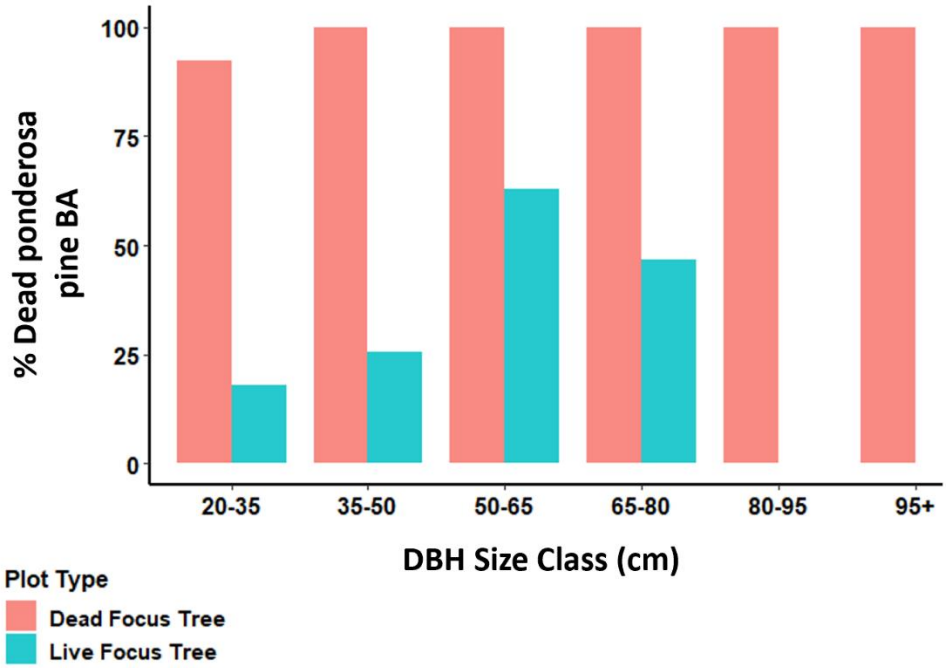

Fig. 2-4 Percentage of ponderosa pine basal area that died during the recent drought and beetle outbreak in surviving and dead focus tree plots based on DBH size class. For each DBH size class, all trees of that size from dead (red) and surviving (blue) focus tree plots were included, and percentage of dead basal area was calculated. Focus tree basal area is not included in this figure.

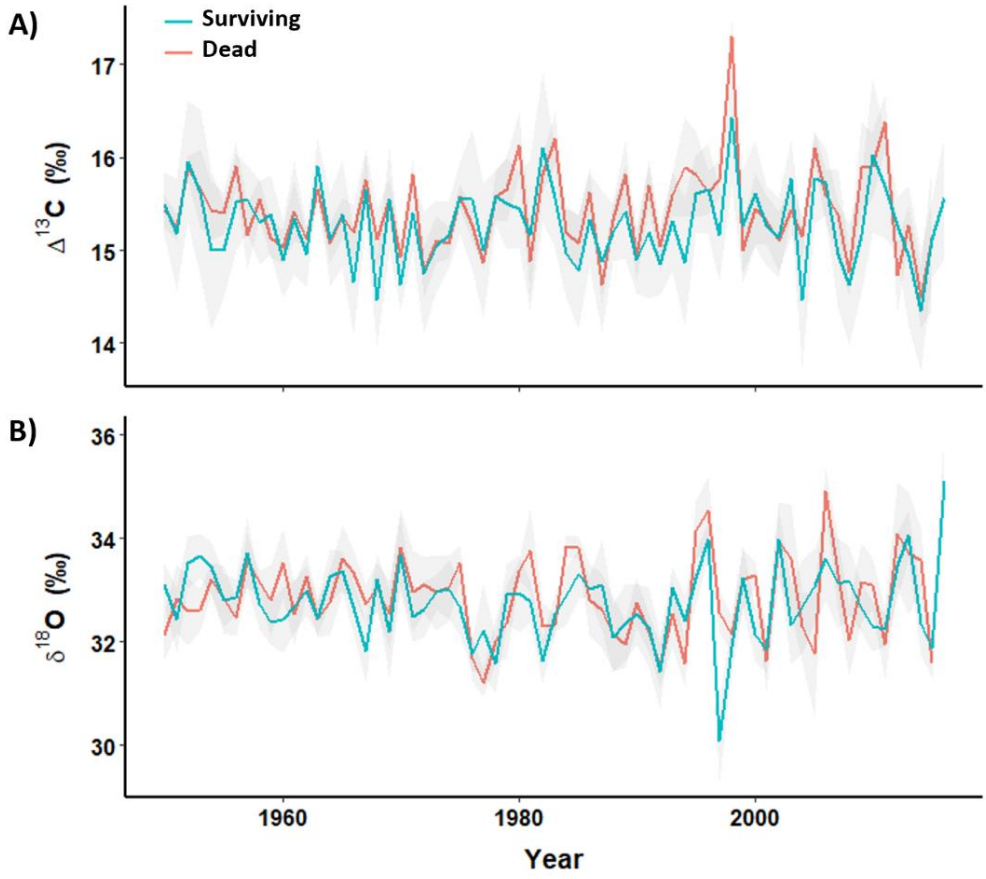

Fig. 2-5 Pre-whitened latewood $\Delta^{13}C$ (A) and $\delta^{18}O$ (B) data for the years 1950-2016 separated by focus tree status (dead or surviving). Error ribbons for each record represent standard error.

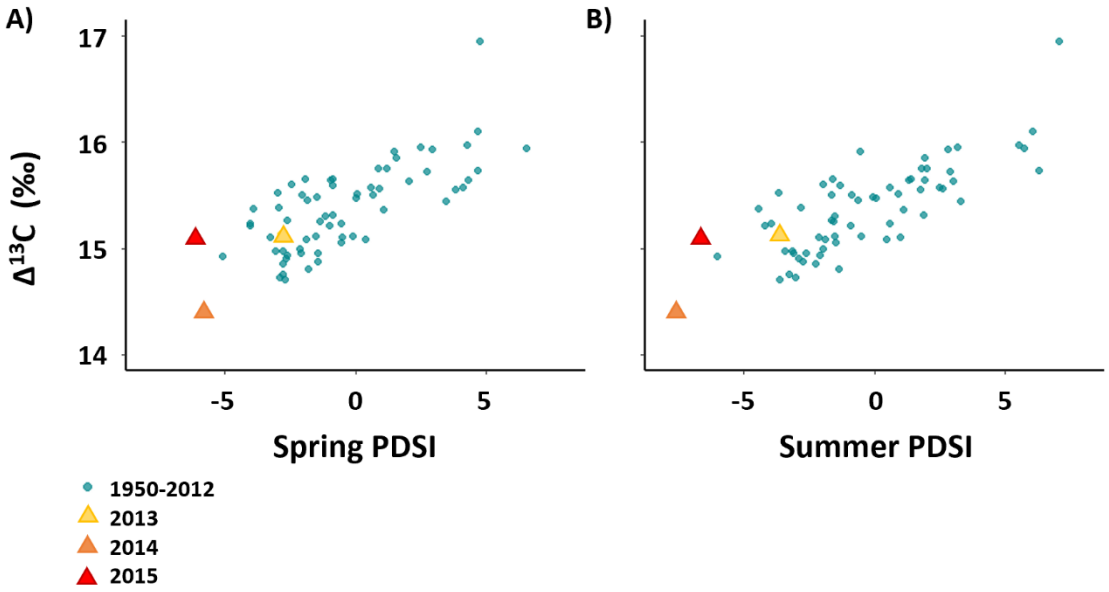

Fig. 2-6 Pre-whitened spring (A) and summer (B) PDSI compared to latewood $\Delta^{13}C$ values from 1950-2015. Drought years are represented by triangles (2013 in yellow, 2014 in orange, 2015 in red). All other years (1950-2012) are represented by blue circles.

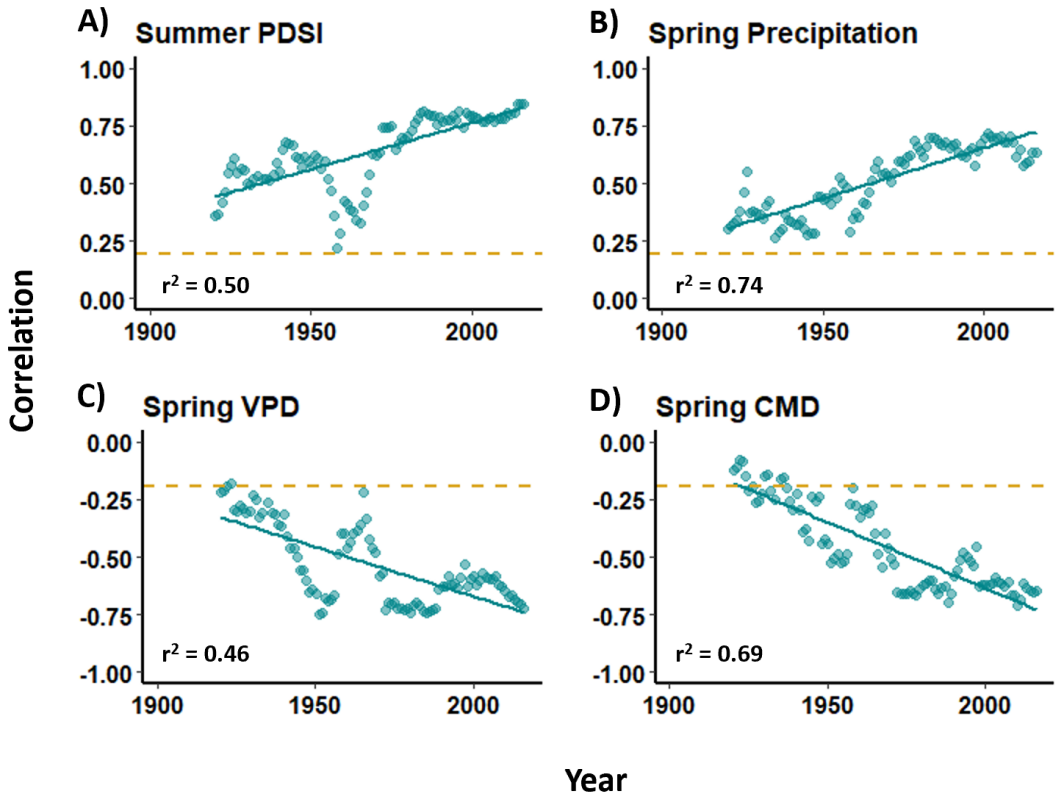

Fig. 2-7 20-year moving window correlations for $\Delta^{13}C$ with (A) summer PDSI, (B) spring precipitation, (C) spring VPD, and (D) spring CMD. Pre-whitened isotope data (including surviving and dead focus trees) was compared to residual climate data for the years 1900-2016. Linear trendlines were fit to each plot and r^2 values are included in each panel. Yellow dashed lines represent the correlation significance cutoff – significant correlations are ≥ 0.19 or ≤ -0.19.

CHAPTER 3

OPPOSING RESPONSES OF TREE-LEVEL AND ECOSYSTEM-LEVEL WATER USE EFFICIENCY TO VAPOR PRESSURE DEFICIT DURING THE 2012-2015 CALIFORNIA DROUGHT

Abstract

Over the past several decades, increasing temperatures and aridity due to climate warming have resulted in more frequent and severe droughts in the western United States. These changes are also affecting the timing and magnitude of snowpack and spring snow-melt, which in turn has increased hydrological extremes in California. As atmospheric CO_2 continues to rise, understanding ecosystem carbon and water fluxes, and the potential to mediate climate warming via carbon sequestration in forests, has remained an active area of research. However, the relationships between tree- and ecosystem-level carbon and water fluxes are not well understood, and scaling between these levels can be tricky. In this study, we compared ponderosa pine tree-ring measurements (growth rates and stable carbon isotopes; $\Delta^{13}C$) to flux tower measurements of evapotranspiration, gross primary productivity, and water use efficiency in the southern Sierra Nevadas during the unprecedented 2012-2015 California drought. The goal of this study was to determine the extent to which tree-rings recorded ecosystem-scale carbon and water fluxes, and whether tree-level growth rates and stable isotopes can be used to estimate ecosystem-scale evapotranspiration. We found that tree- and ecosystem-scale water use

efficiency had opposite relationships with vapor pressure deficit during this drought event and, therefore, had a strong negative relationship with each other. Tree-ring $\Delta^{13}C$ recorded the opposite signal of ecosystem-scale water use efficiency in this ecosystem, likely due to the contrasting responses of transpiration (via stomatal closure) and soil/surface water evaporation to increasingly severe drought conditions. Nonetheless, due to the strong positive relationship between growth rates and ecosystem-scale gross primary productivity and the strong negative relationship between tree- and ecosystem-level water use efficiency, the annually resolved ratios of tree-ring growth to tree-level water use efficiency were able to accurately predict ecosystem-scale evapotranspiration at this site for the years 2011-2015.

Introduction

Over the past several decades, increasing temperatures and aridity due to climate warming have resulted in more frequent and severe droughts in the western United States (Allen *et al* 2010) and worldwide (Zhou *et al* 2019). These changes, caused predominantly by rising levels of atmospheric CO_2, are also affecting the timing and magnitude of snowpack and spring snow-melt (Gleick 1987, Stewart *et al* 2004, Knowles and Cayan 2004, Mote *et al* 2005), which in turn has increased hydrological extremes in California (Yoon *et al* 2015a). Another consequence of great concern is the increased length of the snow-free season which, combined with greater climate variability,

promotes a greater likelihood of wildfires (Westerling *et al* 2006, Yoon *et al* 2015a). A substantial number of people are potentially impacted by changes to hydrologic regimes, since over 50% of California's annual water supply comes from gradual melting of winter snowpack in the spring (Schwartz and Hall 2017), creating surface runoff and recharging soil moisture before the summer drought period (Barnett *et al* 2005). As atmospheric CO_2 continues to rise and the climate continues to warm, understanding the potential to mediate both effects through carbon sequestration in forests has been an active area of research for decades (Friedlingstein *et al* 1995, Norby and Luo 2004, Voelker *et al* 2006, Pan *et al* 2011, Reichstein *et al* 2013). Hence, the relationship between carbon and water fluxes in forests, or their water use efficiency (WUE), is also of great interest, as shifts in WUE due to rising CO_2 and drought will have implications for both carbon sequestration and hydrologic regimes (De Kauwe *et al* 2013, Keenan *et al* 2013, Voelker *et al* 2016, Keeling *et al* 2017, Medlyn *et al* 2017).

Ecosystem fluxes across the world can be observed and analyzed using tower-based eddy covariance flux measurements (Keenan *et al* 2013, Knauer *et al* 2017, Mastrotheodoros *et al* 2017). However, these flux towers often have a relatively small footprint, and many do not record flux data over long periods of time (Belmecheri *et al* 2014). As a result, our understanding of ecosystem fluxes is often limited both spatially and temporally. Remote sensing can allow flux measurements to be scaled up for large-scale assessments (Schimel *et al* 2014). However, tree-ring growth and stable isotope measurements have the potential to provide more mechanistic insights on how climatic controls over WUE may change across landscapes and forest structures, and through time

(Thomas *et al* 2013, Voelker *et al* 2014, Saurer *et al* 2014, Voelker *et al* 2018, Giguere-Croteau *et al* 2019). These tree-ring characteristics also give insight into tree-level carbon fixation and transpiration, and their relationships to ecosystem-level flux measurements. Moreover, tree-rings can be efficiently collected across forested landscapes and extend far back in time across a much greater range of past climate and atmospheric CO_2 variability.

Tree-ring growth and stable isotopes can provide valuable and complementary information to flux measurements. Tree-rings may also potentially serve as powerful proxies for both carbon and water ecosystem flux measurements. Hence, in combination, tree-ring and flux measurements could yield novel insights into historical flux variability and important spatial information across landscapes. Several studies have compared ecosystem carbon production to tree-ring basal area increment (BAI) (Babst *et al* 2014a, Rocha *et al* 2006, Barford *et al* 2001) and ring width index (RWI) (Babst *et al* 2014b, Dye *et al* 2016, Klesse *et al* 2016, Teets *et al* 2018, Tei *et al* 2019), but only a handful of studies have explored the relationship between tree-ring stable isotopes and ecosystem flux measurements (Belmecheri *et al* 2014, Michelot *et al* 2011, Yi *et al* 2018, Tei *et al* 2019). In this study, we hope to improve our understanding of how tree-level measurements can record ecosystem carbon and water fluxes in a dry, mixed-conifer forest in the southern Sierra Nevada Mountains during the unprecedented "California drought" (2012-2015).

Flux tower data from Soaproot Saddle, a Southern Sierra Critical Zone Observatory (SSCZO) site in the southern Sierra Nevadas, CA (figure 3-1), provided

ecosystem flux data for the years 2011-2015. In this study, we compare that flux data to intra-annual $\Delta^{13}C$ (carbon isotope discrimination) and growth rates (basal area increment; BAI) during the same time period. This time span encompasses the 2012-2015 California drought (hereafter referred to as the "CA Drought"), a multi-year period of low precipitation and unusually high temperatures that resulted in severe drought conditions (Griffin and Anchukaitis 2014) and widespread forest mortality (Fettig *et al* 2019, Pile *et al* 2019). High winter temperatures (particularly in water year 2014) and low winter precipitation greatly reduced snowpack and spring snow-melt, resulting in very little soil-water recharge for several years in a row (Shukla *et al* 2015).

The severity of the CA Drought, and the availability of flux data from the SSCZO, provided a unique opportunity to observe seasonality of canopy-scale evapotranspiration (ET), gross primary productivity (GPP), and water use efficiency (WUE), and to compare that flux data to intra-annual tree-ring characteristics including growth rates and $\Delta^{13}C$ of alpha-cellulose. At the tree-level, linkages between water and carbon cycling are typically controlled by stomatal conductance, as it is the primary plant response to drought stress and largely constrains transpiration and photosynthetic carbon assimilation across tree canopies (Farquhar *et al* 1989, McCarroll and Loader 2004, Ehleringer and Farquhar 1993). Water use efficiency at the ecosystem level is defined by the ratio of GPP to ET, or the ratio of carbon gained to water lost, and is described by the following equation:

(1) $$WUE = \frac{GPP}{ET}$$

Two additional measures of ecosystem-scale water use efficiency, inherent WUE (IWUE) (Beer *et al* 2009) and underlying WUE (uWUE) (Zhou *et al* 2014), include vapor pressure deficit (VPD) to account for its influence on stomatal conductance (Oren *et al* 1999). These relationships are described by the following equations:

(2) $$uWUE = GPP * \frac{VPD^{0.5}}{ET}$$

(3) $$IWUE = GPP * \frac{VPD}{ET}$$

These different measures of water use efficiency are typically used when assessing carbon and water fluxes on different time scales – WUE is consistent at monthly time scales (Yang *et al* 2013), but VPD has been shown to have a large effect on water use efficiency at shorter time scales (Abbate *et al* 2004, Zhao *et al* 2005, Hu *et al* 2008). IWUE is typically more accurate at daily timescales, and uWUE is more accurate at hourly or half-hourly timescales (Zhou *et al* 2014, Zhou *et al* 2015). Only two studies that we are aware of have used ecosystem flux data to compare water use efficiency variables to tree-ring stable carbon isotopes (Michelot *et al* 2011, Yi *et al* 2018), and both were conducted in temperate climates as opposed to the strong Mediterranean climate in the southern Sierra Nevadas. In this study, we compare ecosystem-scale WUE, uWUE, and IWUE measurements to intra-annual tree-ring growth (BAI) and carbon isotope discrimination ($\Delta^{13}C$) to evaluate whether these tree-level measurements can be utilized to predict ecosystem-scale fluxes

Carbon isotope discrimination ($\Delta^{13}C$), like water use efficiency, is largely controlled by stomatal conductance and photosynthetic rate (Farquhar *et al* 1982,

Ehleringer *et al* 1993, McCarroll and Loader 2004). In ponderosa pines, stomatal conductance typically decreases when drought stress increases, resulting in less discrimination against the heavier isotope (^{13}C) during carbon fixation (Roden and Ehleringer 2007, Voelker *et al* 2018). $\Delta^{13}C$ is also linearly related to the ratio of intra-cellular and atmospheric CO_2 concentrations (c_i and c_a, respectively) (Farquhar *et al* 1982, McCarroll and Loader 2004). This relationship is described in the following equation (Farquhar *et al* 1982):

$$\Delta^{13}C = a + (b - a)(c_i/c_a) \quad (4)$$

where *a* represents discrimination against ^{13}C during diffusion through the stomata (-4.4 ‰), and *b* represents discrimination against ^{13}C during carboxylation (-27 ‰) (McCarroll and Loader 2004). This relationship between $\Delta^{13}C$ and c_i/c_a can be used to calculate intrinsic water use efficiency (iWUE), which is the ratio of photosynthetic carbon assimilation (A) to stomatal conductance (g_s) (McCarroll and Loader 2004):

$$iWUE = A/g_s = c_a[1 - (c_i/c_a)] * 0.625 \quad (5)$$

Comparing iWUE to measures of ecosystem-scale water use efficiency derived from flux tower measurements (WUE, uWUE, and IWUE) will allow us to determine to what extent, if any, $\Delta^{13}C$ and associated iWUE matches ecosystem-scale carbon and water cycling during seasonal and inter-annual drying events.

In this study, intra-annual tree-ring growth and $\Delta^{13}C$ were compared to ecosystem flux data from Soaproot Saddle, an SSCZO site in the central Sierras with a strong Mediterranean climate. Data from 2011-2015, encompassing the 2012-2015 California

drought, was analyzed and compared to tree-ring characteristics of ponderosa pines within the flux tower footprint. The main objectives of this study were to determine (1) how ET, GPP, and water use efficiency changed over the course of the drought, (2) the extent to which tree-ring $\Delta^{13}C$ recorded ecosystem carbon and water fluxes at this site, and (3) whether ecosystem-scale ET could be reconstructed using tree-ring growth and $\Delta^{13}C$ data.

Methods

Study area and field data collection

Sampling for this study took place at Soaproot Saddle, a Southern Sierra Critical Zone Observatory (SSCZO) site in the central Sierra Nevadas (figure 3-1). The same paired plots and focus tree cores described in chapter 2 were used in this study for higher-temporal resolution sampling for the years 1997-2016. For more information on plot locations and structure, see Chapter 2 methods (pages 20-21) and figure 2-2. Samples were collected within the footprint of the on-site flux tower at Soaproot Saddle. A portion of Big Creek, a perennial stream, runs through the flux tower footprint and was flowing when sampling was conducted in March of 2017.

Increment core preparation and measurement

Cores from each focus tree were prepared as described in Chapter 2 methods (pages 21-22) – whole ring as well as separate latewood and earlywood ring widths were measured using MeasureJ2X software (Coortech Consulting) and visual crossdating was validated with COFECHA (Holmes 1983). Ring width chronologies were each detrended using a 100-year spline in ARSTAN (Bunn 2008) to isolate climate trends. Ring widths were measured from the most current year of growth back to 1997. DBH and ring widths were used to calculate whole ring, earlywood, and latewood basal area increment (BAI) for each focus tree to determine annual growth rates. BAI was calculated from the outside-in, assuming circularity of the growing cambium and employed estimates of bark thickness (McDonald 1983, Larsen and Hann 1985) to adjust for differences in radial measurements inside and outside of the bark for each tree. BAI values were multiplied by estimated wood specific density for early- and latewood (Bouffier *et al* 2003; earlywood = 0.385, latewood = 0.56), then summed for each year to obtain annual BAI-Index values (BAI_x). These values should be proportional to forest-wide tree carbon fixation among seasons by accounting for wood density as well as across years by assuming any potential changes in forest density, tree height, and allometry are inconsequential when assessed over the five years in which tree-rings and flux data are compared for this study (2011-2015).

Stable isotope analyses

For this portion of the study, only the years 1997-2016 were used for isotope analysis in order to conduct higher temporal resolution sampling of annual rings. Each ring was divided into early-, middle-, and latewood with a scalpel under a dissecting microscope. Each of these ring portions were ground into a fine powder and sealed in a mesh filter bag before being bleached to isolate α-cellulose (bleaching and homogenization methods described in Chapter 2; page 22-24). Samples were then dried and packed into tin ($\Delta^{13}C$) capsules before being analyzed on a mass spectrometer at the Center for Isotope Biogeochemistry (CSIB) at the University of California, Berkeley (for details regarding equipment and precision, see Chapter 2 methods section; page 24). All reported $\delta^{13}C$ values were converted to carbon isotope discrimination values ($\Delta^{13}C$) following Farquhar *et al* (1982) using $\delta^{13}C_{air}$ records from Moana Loa, Hawaii (see Chapter 2 methods; page 24).

Raw $\Delta^{13}C$ isotope series were detrended in ARSTAN (Cook and Krusik 2014) using a 100-year spline to isolate inter-annual climate trends and remove low-frequency variation that could be due to rooting depth, tree height, or competition. Pre-whitened series were then multiplied by the mean $\Delta^{13}C$ value for each core, resulting in detrended isotope series with autocorrelation removed for each focus tree for the years 1997-2016. A repeated measures mixed effects model (nlme package in R; Pinheiro *et al* 2016) was used to determine whether ring portions (early-, middle-, and latewood) were significantly different from one another. In this model, $\Delta^{13}C$ was the response variable, ring portion was the predictor, and focus tree pair was included as a random variable.

Intra-annual $\Delta^{13}C$ was also used to calculate intrinsic water use efficiency (iWUE) using equation (4).

Climate data analysis

Vapor pressure deficit (VPD) data for Soaproot Saddle (37.031° -119.256°) were obtained through PRISM (http://prism.oregonstate.edu/) for the years 2011-2015. Eddy covariance measurements from the Soaproot Saddle flux tower, including incoming solar radiation (*K*), and net ecosystem exchanges of water (evapotranspiration; ET) and CO_2 (net ecosystem exchange; NEE), were provided by the SSCZO (Goulden *et al* 2006). Respiration was calculated at 10-day intervals and added to NEE to produce monthly gross primary productivity (GPP) data for the years 2011-2015 (Goulden *et al* 2006, Goulden *et al* 2012). To obtain continuous datasets for each of the monthly ET, VPD, and GPP variables, Gaussian curves were fit to the data after months had been converted to day of year. The relationships used the following form:

(6) $$y = y_o + ae^{[-0.5\left(\frac{x-x_0}{b}\right)^2]}$$

Where *y* is the predictand, *x* is day of year, y_0 is the lowest estimated baseline value of *y*, x_0 is the timing of the estimated peak during the year, and *a* and *b* are parameters controlling curvature of the peaking relationship.

Daily estimates of ET, VPD, and GPP data were used to calculate daily water use efficiency (WUE), underlying water use efficiency (uWUE), and inherent water use efficiency (IWUE) for the years 2011-2015 (equations (1), (2), and (3) respectively).

iWUE derived from early-, middle-, and latewood $\Delta^{13}C$ was then compared to seasonal VPD, WUE, uWUE, and IWUE. Pearson's correlation coefficients were calculated, and regression analyses were performed for each combination to determine strength of relationship.

Climate variables (ET, VPD, GPP, and ecosystem-scale WUE variables) were averaged by season for comparison to intra-annual iWUE data, which were derived from early-, middle-, and latewood $\Delta^{13}C$. Earlywood values were compared to spring climate data (March, April, May), latewood values were compared to summer climate data (June, July, August), and middlewood values were compared to an average of the spring and summer climate conditions as defined above.

Evapotranspiration estimate

By rearranging equation (1), it can be determined that ET should be a function of GPP/WUE and be predictable based on the relationship between tree-ring growth and GPP, as well as the relationship between iWUE and WUE. Toward this end, for the years 2011-2015, we determined whether growth rate was related to GPP on an interannual basis by comparing early- and latewood BAI_x values to seasonal GPP using a linear regression analysis. We used the same approach for comparing iWUE and WUE. ET was then estimated using BAI_x and iWUE (derived from $\Delta^{13}C$ values) as proxies for ecosystem-scale GPP and WUE, respectively, using the following equation:

(7) $$ET = BAI\ Index/iWUE$$

Estimated ET was compared to flux tower measurements of ET for the years 2011-2015 using a regression analysis.

Results

During the years 1997-2016, early-, middle-, and latewood $\Delta^{13}C$ showed a distinct intra-annual pattern, whereby earlywood consistently had the highest $\Delta^{13}C$ values, followed by middlewood, then latewood (figure 3-2). Comparisons among intra-annual components showed significantly different ($p < 0.001$) $\Delta^{13}C$ values for all combinations. Similarly, earlywood BAI was significantly greater than latewood BAI ($p < 0.01$) for the years 1997-2016. Earlywood, latewood, and whole ring BAI declined at the onset of the 2012-2015 California Drought (figure 3-3), but rebounded to some extent, particularly in latewood, following the end of the drought in 2015.

Data from the SSCZO flux tower for the years 2011-2015 showed that peak ET and GPP shifted earlier in the growing season as the drought progressed, while the timing of VPD peaks stayed relatively constant (figure 3-4(a)-(c)). Peak ET values also decreased in magnitude each year as the drought progressed, most notably between 2012 and 2013 (figure 3-4(a)). WUE, uWUE, and IWUE over the course of the drought are shown in figure 3-4(d)-(f).

$\Delta^{13}C$ data was used to calculate intrinsic water use efficiency (iWUE) (equation (4)), and iWUE values were compared to VPD for the years 2011-2015. iWUE had a

strong positive relationship with VPD (correlation = 0.93, R^2 = 0.86), while ecosystem-scale WUE had a strong negative relationship with VPD (correlation = -0.94, R^2 = 0.89) (figure 3-5; figure B-1). iWUE was also compared to ecosystem WUE, uWUE and IWUE. iWUE was negatively related to WUE (correlation = -0.94, R^2 = 0.88) and uWUE (correlation = -0.82, R^2 = 0.67). In contrast to the negative relationships between iWUE and each of WUE and uWUE, iWUE had a positive relationship with IWUE. However, the correlation was weak (0.48) and the relationship was not significant (p = 0.07) (figure 3-6).

Seasonal GPP was also compared to annual growth rates using BAI_x values (i.e., intra-annual BAI corrected for wood density fluctuations between early- and latewood). The strongest relationships were achieved when earlywood BAI_x values were compared to the sum of spring/summer GPP (Mar-Aug) and latewood BAI_x values were compared to the sum of summer/fall GPP (July-Oct). Regression analyses for earlywood BAI_x and spring/summer GPP (correlation = 0.94; R^2 = 0.88) and for latewood BAI_x and summer/fall GPP (correlation = 0.93; R^2 = 0.87) were both significant (p = 0.02 in both cases). The sum of early- and latewood BAI_x was then calculated for each year. Similarly, the sum of growing season (Mar-Oct) GPP was calculated for each year. Regression analysis showed a strong positive relationship between BAI_x annual sums and GPP growing season sums for the years 2011-2015 (correlation = 0.87; R^2 = 0.90; p = 0.01) (Figure 3-7(a)).

Following equation (5), the ratio of BAI_x to iWUE was then compared to measured ecosystem-scale ET from the SSCZO flux tower. Regression analysis showed

that these two variables had a strong positive relationship ($R^2 = 0.99$, $p < 0.01$). In turn, the resulting predictions of ET from BAI_x/iWUE were strongly related to ecosystem-scale ET, yielding an R^2 value of 0.99 and a slope of 0.99 (figure 3-7(b)).

Discussion

As the CA Drought progressed, peak ET and GPP shifted earlier in the year, indicating an earlier start to the growing season and earlier onset of summer drought stress (figure 3-4(a)-(b)). Peak ET also decreased during the drought, likely due to progressively severe drought stress, increasing stomatal closure, lower soil evaporation and, eventually, canopy tree mortality within the flux tower footprint. Across much of California, Asner *et al* (2015) showed that canopy drought stress became increasingly severe over the course of the drought, resulting in widespread mortality. Due to increasing stomatal constraints on leaf gas exchange and the high ponderosa pine mortality rate in this part of California, particularly in later part of the drought (i.e., ~89% of overstory ponderosa pines; Fettig *et al* 2019, Pile *et al* 2019), the impact on both ET and GPP were prodigious. Our primary interest in this study was to determine the extent to which intra-annual tree-ring growth and $\Delta^{13}C$ measurements recorded ecosystem-scale carbon and water flux dynamics and their combined estimates of ET leading up to this mortality event that occurred near the end of the CA Drought.

iWUE, derived from tree-ring $\Delta^{13}C$, had a strong positive relationship with VPD while ecosystem-scale WUE had the opposite response during the drought. In seasonally dry climates like that of southern California, higher iWUE (associated with lower $\Delta^{13}C$) during warmer, drier growing conditions is expected due to decreased stomatal conductance and transpiration relative to photosynthetic carbon assimilation (McCarroll and Loader 2004, Roden and Ehleringer 2007, Voelker *et al* 2019). However, these leaf-level and canopy-integrated physiological processes do not always reflect ecosystem-scale carbon and water fluxes (Jarvis and McNaughton 1986), as was the case in this study. Although iWUE had the expected relationship with VPD, the opposite trend was seen at the ecosystem scale – higher ecosystem WUE during periods of lower VPD. This counter-intuitive relationship has been observed in other studies (Reichstein *et al* 2007, Beer *et al* 2009, Reichstein *et al* 2002, Jiang *et al* 2019 *in review*) and is likely a result of other important processes (aside from canopy gas exchange) occurring within the flux tower footprint, including evaporation of soil moisture and stream water (Jarvis and McNaughton 1986, Law *et al* 2000).

Currently, partitioning ET into evaporation (E) and transpiration (T) is difficult at the ecosystem scale (Stoy *et al* 2019). In many cases, ecosystem ET is assumed to be nearly 100% T (T/ET = 1), with little input from evaporation of other water sources, but this is not the case in all ecosystems (Stoy *et al* 2019). Stoy *et al* (2019) notes that studies in Mediterranean ecosystems have found non-zero E/ET values even during dry summer months, suggesting that evaporation of soil and/or surface water could be contributing to ecosystem ET throughout the growing season. Specifically, Perez-Preigo *et al* (2018)

found that soil E/ET ranged from 0.3 to 0.8 in a Mediterranean savannah ecosystem, indicating that soil evaporation can remain a substantial component of ecosystem ET even under dry conditions. In a ponderosa pine-dominated forest in Oregon, Law *et al* (2000) modeled soil moisture evaporation to range from about 0.5 to 1.25 mm per day. At Soaproot Saddle, soil evaporation rates would be expected to be greater due to higher temperatures (by ~5 °C) and 40 cm greater precipitation compared to the Law *et al* (2000) flux site in Oregon. Moreover, a portion of Big Creek is located only 35 m from the flux tower and flows across much of the tower footprint at Soaproot Saddle, which also would have bolstered ecosystem evaporation, particularly during the summer. Indeed, the effect of soil drying on GPP, which is tied directly to stomatal conductance through Fick's law (Farquhar *et al* 1989), started earlier and was comparatively greater compared to the effect of soil drying on ET, which indicates that soil evaporation was an increasingly large component of ET during progressively drier conditions at this flux site (Figure B-1). Taken together, these patterns in flux responses help explain the strong negative relationship between tree-level iWUE and ecosystem-scale WUE at this site.

The relationship between iWUE and uWUE was not as strong, and the relationship between iWUE and IWUE was particularly weak. Both IWUE and uWUE are assessed at the ecosystem-level and have previously been employed at finer time scales (daily, hourly, half-hourly) at which VPD has strong effects on variation in fluxes due to the responsiveness of stomata to atmospheric evaporative demand (Abbate *et al* 2004, Zhao *et al* 2005, Hu *et al* 2008, Zhou *et al* 2015). However, iWUE derived from intra-annual $\Delta^{13}C$ data is at a much coarser time scale that spans months rather than

minutes to hours. At the ecosystem level, WUE has been used more often when summarizing carbon and water fluxes on monthly time-scales (Yang *et al* 2013, Zhou *et al* 2015), which agrees with our results that ecosystem-level WUE is more closely tied to tree-level iWUE when considering time scales of months to full growing seasons.

Another potential contributor to the observed discordance between responses of iWUE and WUE to VPD is cloud cover and its effect on carbon and water fluxes, particularly when ecosystem scale fluxes include substantial soil and/or stream water evaporation. In the Mediterranean climate at Soaproot Saddle, higher cloud cover and lower VPD typically occur during cool and wet spring seasons while lower cloud cover and higher VPD typically occur during warmer, drier summer seasons. Higher cloud cover has been shown to increase photosynthetic carbon assimilation due to the prominence of diffuse radiation, which is used more efficiently by plant canopies (Gu *et al* 2002, Still *et al* 2009, Zhang *et al* 2011). However, at the ecosystem scale, cloud cover not only affects transpiration from vegetation, but also evaporation from soil moisture and surface waters, such as Big Creek. As a result, ecosystem ET would increase markedly during sunny conditions due to soil and stream water evaporation, despite a decrease in stomatal conductance in canopy trees. In this way, ecosystem-scale WUE at Soaproot Saddle would tend to be higher during cloudy conditions (high photosynthetic carbon assimilation, relatively low ET) and lower during sunny conditions (lower carbon assimilation due to stomatal constraints, high ET due to soil and stream water evaporation). Indeed, a recent study by Jiang *et al* (*in review*) also found that ecosystem-scale WUE was higher during periods of higher cloud cover in an old growth coniferous

forest occurring in a Mediterranean climate in southern Washington. Conversely, tree-level iWUE would not be affected by soil and stream water evaporation because it is primarily controlled by stomatal conductance (Farquhar *et al* 1982, Ehleringer *et al* 1993, McCarroll and Loader 2004). In general, stomatal conductance is higher during cool, wet conditions and lower during warm, dry conditions (Oren *et al* 1999, McCarroll and Loader 2004). During warm, dry conditions, stomata close to reduce water lost via transpiration, which increases WUE relative to cooler, wetter conditions. Together, these factors help explain the opposite relationships of iWUE and WUE with VPD shown in Figure 3-4.

It is likely that the negative relationship found between ecosystem-scale WUE and VPD is a result of the strong Mediterranean climate at Soaproot Saddle, where summer precipitation is very low, and temperatures are high. In more temperate climates, precipitation is more evenly distributed throughout the year and summer droughts are much less pronounced. A study by Yi *et al* (2018), which took place in a temperate deciduous forest in Indiana, found a positive relationship between ecosystem-scale WUE and VPD, while we found the opposite relationship at Soaproot Saddle (Figure 3-5(b)). It appears that the presence of strong summer drought conditions at Soaproot Saddle may result in the negative relationships of ecosystem-scale WUE with both VPD and iWUE. Our results, and those of Jiang *et al* (*in review*) suggest that opposing responses of iWUE and WUE to VPD may be a commonality in Mediterranean climates, with the strength of this discordance among tree- and ecosystem-level water use efficiency being related to the local soil and geomorphic conditions. Given the contrasting results among studies

located in summer-wet versus summer-dry environments, we suspect that there is a transition of iWUE vs. WUE that depends on the growing season water balance of the ecosystem. However, there is not yet enough data to test this hypothesis.

In addition to the strong negative relationship between iWUE and WUE at Soaproot Saddle, intra-annual growth rates (BAI_x) had a strong positive relationship with ecosystem-scale GPP. This indicates that higher carbon uptake in this ecosystem is associated with higher rates of growth in large canopy trees. This relationship has been observed in several other studies looking at ecosystem CO_2 flux compared to BAI (Babst *et al* 2014a, Rocha *et al* 2006, Barford *et al* 2001) and ring width index (RWI) (Babst *et al* 2014b, Dye *et al* 2016, Klesse *et al* 2016, Teets *et al* 2018, Tei *et al* 2019). Given the strength of this relationship, and our ability to calculate iWUE from tree-ring $\Delta^{13}C$, we also explored the potential to use tree-ring growth and iWUE to estimate ecosystem-scale ET. Results showed that ET estimated using the ratio of BAI_x /iWUE was highly correlated with ecosystem-scale ET measured at the SSCZO flux tower when summed across each year (Figure 3-7(b)). In other regions or sites where iWUE is not as strongly related to ecosystem-scale WUE it will not be possible to reconstruct ET from tree-ring growth and $\Delta^{13}C$. Alternatively, in summer-wet locations where iWUE and ecosystem-scale WUE are positively related, it may be possible to use this approach even though the sign of the relationship is the opposite to that observed at Soaproot Saddle. Therefore, further research into the ability to estimate ET using this approach is needed to determine feasibility under various combinations of climates and geomorphological conditions.

Conclusion

The ability to utilize tree-ring measurements to estimate ecosystem carbon and water fluxes back in time would be extremely valuable, particularly in areas where flux towers are absent, or where flux data is only available for a short period of time. Recent studies have also found strong links between tree growth and/or stable isotopes and other ecosystem-scale variables, including GPP (Babst *et al* 2014a, Belmecheri *et al* 2014) and NPP (Voelker 2011, Levesque *et al* 2019), further suggesting the potential for combining tree-ring growth and stable isotopes to reconstruct and predict ecosystem carbon and water fluxes across diverse ecosystems. The CA Drought provided a unique opportunity to compare tree- and ecosystem-level carbon and water fluxes during a period of extreme drought, and thereby has provided valuable insight into this relationship for mid-elevation forests of the southern Sierra Nevadas. Further research of this kind across diverse ecosystems will be necessary to determine the widespread utility of tree-ring measurements for reconstructing past ecosystem-scale carbon and water fluxes.

References

Abbate PE, Dardanelli JL, Cantarero MJ, Maturanoc M, Melchiorid RJM and Sueroa EE 2004 Climatic and water availability effects on water-use efficiency in wheat *Crop Sciences.* **44** 474–483

Allen CD *et al* 2010 A global overview of drought and heat-induced tree mortality reveals emerging climate change risks for forests *Forest Ecology and Management* **259** 660-684

Asner GP, Martin RE, Anderson CB and Knapp DE 2015 Quantifying forest canopy traits: Imaging spectroscopy versus field survey *Remote Sensing of Environment* **158** 15-27

Babst F, Bouriaud O, Papale D, Gielen B, Janssens IA, Nikinmaa E, Ibrom A, Wu J, Bernhofer C, Köstner B and Grünwald T 2014a Above-ground woody carbon sequestration measured from tree rings is coherent with net ecosystem productivity at five eddy-covariance sites *New Phytologist* **201** 1289-303

Babst F *et al* 2014b A tree-ring perspective on the terrestrial carbon cycle *Oecologia* **176** 307-22

Barford CC, Wofsy SC, Goulden ML, Munger JW, Pyle EH, Urbanski SP, Hutyra L, Saleska SR, Fitzjarrald D and Moore K 2001 Factors controlling long-and short-term sequestration of atmospheric CO_2 in a mid-latitude forest *Science* **294** 1688-1691

Barnett TP, Adam JC and Lettenmaier DP 2005 Potential impacts of a warming climate on water availability in snow-dominated regions *Nature* **438** 303–309

Beer C *et al* 2009 Temporal and among-site variability of inherent water use efficiency at the ecosystem level *Global biogeochemical cycles* **23** 10.1029/2008GB003233

Belmecheri S, Maxwell RS, Taylor AH, Davis KJ, Freeman KH and Munger WJ 2014 Tree-ring $\delta^{13}C$ tracks flux tower ecosystem productivity estimates in a NE temperate forest *Environmental Research Letters* **9** 074011

Bouffier LA, Gartner BL and Domec JC 2007 Wood density and hydraulic properties of ponderosa pine from the Willamette valley vs. the Cascade mountains *Wood Fiber Science* **35** 217–233

Bunn AG 2008 A dendrochronology program library in R (dplR) *Dendrochronologia* **26** 115-124

Cook ER and Krusic PJ 2014 ARSTAN version 44h3: A tree-ring standardization program based on detrending and autoregressive time series modeling, with interactive graphics. Tree-Ring Laboratory, Lamont-Doherty Earth Observatory of Columbia University, Palisades, New York, USA

De Kauwe MG *et al* 2013 Forest water use and water use efficiency at elevated CO_2: a model-data intercomparison at two contrasting temperate forest FACE sites *Global Change Biol*ogy **19** 1759-1779

Dye A, Plotkin AB, Bishop D, Pederson N, Poulter B and Hessl A 2016 Comparing tree-ring and permanent plot estimates of aboveground net primary production in three eastern US forests *Ecosphere* **7** e01454.10.1002/ecs2.1454

Ehleringer JR, Hall AE and Farquhar GD 1993 *Stable Isotopes and Plant Carbon–Water Relations* (New York: Academic Press)

Farquhar GD, O'Leary MH and Berry JA 1982 On the relationship between carbon isotope discrimination and intercellular carbon dioxide concentration in leaves *Australian Journal of Plant Physiology* **9** 121–137

Farquhar GD, Ehleringer JR and Hubick KT 1989 Carbon isotope discrimination and photosynthesis *Annu. Rev. Plant Physiol. Plant Mol. Biol.* **40** 503-537

Fettig CJ, Mortenson LA, Bulaon BM and Foulk PB 2019 Tree mortality following drought in the central and southern Sierra Nevada, California, US *Forest ecology and Management* **432** 164-78

Friedlingstein P, Fung I, Holland E, John J, Brasseur G, Erickson D and Schimel D 1995 On the contribution of CO2 fertilization to the missing biospheric sink *Global Biogeochem. Cycles* **9** 541–55

Giguère-Croteau C, Boucher É, Bergeron Y, Girardin MP, Drobyshev I, Silva LC, Hélie JF and Garneau M 2019 North America's oldest boreal trees are more efficient water users due to increased [CO2], but do not grow faster *Proceedings of the National Academy of Sciences* 241668

Gleick PH 1987 Regional Hydrologic Consequences of increases in Atmospheric Carbon Dioxide and other Trace Gases *Climatic Change* **10** 137–161

Goulden ML, Anderson RG, Bales RC, Kelly AE, Meadows M and Winston GC 2012 Evapotranspiration along an elevation gradient in California's Sierra Nevada *Journal of Geophysical Research: Biogeosciences* **117** G3

Goulden ML, Winston GC, McMillan AS, Litvak ME, Read EL, Rocha AV and Rob Elliot J 2006 An eddy covariance mesonet to measure the effect of forest age on land-atmosphere exchange *Global Change Biology* **12** 2146–2162

Griffin D and Anchukaitis KJ 2014 How unusual is the 2012-2014 California drought? *Geophysical Research Letters* **41** 9017–9023

Gu L, Baldocchi DD, Verma SB, Black TA, Vesala T, Falge EM and Dowty PR 2001 Advantages of diffuse radiation for terrestrial ecosystem productivities *Journal of Geophysical Research* **107** ACL-2

Holmes RL 1983 Computer-assisted quality control in tree-ring dating and measurement. *Tree Ring Bulletin* **43** 69-78

Hu ZM, Yu GR, Fu YL, Sun XM, Li YN, Shi PL, Wang YF and Zheng ZM 2008 Effects of vegetation control on ecosystem water use efficiency within and among four grassland ecosystems in China *Global Change Biology* **14** 1609–1619

Hu J, Moore DJP, Burns SP and Monson RK 2010 Longer growing seasons lead to less carbon sequestration by a subalpine forest *Global Change Biology* **16** 771–783

Jarvis PG and McNaughton KG 1986 Stomatal control of transpiration: scaling up from leaf to region *Advances in Ecological Research* **15** 1-49

Jiang Y, Still CJ, Rastogi B, Page GFM, Wharton S, Meinzer FC, Voelker S and Kim JB 2019 Trends and controls on water-use efficiency of an old-growth coniferous forest in the Pacific Northwest *Environmental Research Letters* (In Review)

Keeling RF, Graven HD, Welp LR, Resplandy L, Bi J, Piper SC, Sun Y, Bollenbacher A and Meijer HA 2017 Atmospheric evidence for a global secular increase in carbon isotopic discrimination of land photosynthesis *PNAS* **114** 10361-10366

Keenan TF, Hollinger DY, Bohrer G, Dragoni D, Munger JW, Schmid HP and Richardson AD 2013 Increase in forest water-use efficiency as atmospheric carbon dioxide concentrations rise *Nature* **499** 324

Klesse S, Etzold S and Frank D 2016 Integrating tree-ring and inventory-based measurements of aboveground biomass growth: research opportunities and carbon cycle consequences from a large snow breakage event in the Swiss Alps *European journal of forest research* **135** 297-311

Knauer J, Zaehle S, Reichstein M, Medlyn BE, Forkel M, Hagemann S and Werner C 2017 The response of ecosystem water-use efficiency to rising atmospheric CO_2 concentrations: sensitivity and large-scale biogeochemical implications *New Phytologist* **213** 1654-66

Knowles N and Cayan D 2004 Elevational Dependence of Projected Hydrologic Changes in the San Francisco Estuary and Watershed *Climatic Change* **62** 319–336

Law BE, Williams M, Anthoni PM, Baldocchi DD and Unsworth MH 2000 Measuring and modelling seasonal variation of carbon dioxide and water vapour exchange of a *Pinus ponderosa* forest subject to soil water deficit *Global Change Biology* **6** 613-630

Larsen DR and Hann DW 1985 Equations for predicting diameter and squared diameter inside bark at breast height for six major conifers of southwest Oregon *Forest Service Research Laboratory Research Note **77*** (Oregon State University, Corvallis, OR, USA)

Levesque M, Andreu-Hayles L, Smith WK, Williams AP, Hobi ML, Allred BW and Pederson N 2019 Tree-ring isotopes capture interannual vegetation productivity dynamics at the biome scale *Nature Communications* **10** 742

Mastrotheodoros T, Pappas C, Molnar P, Burlando P, Keenan TF, Gentine P, Gough CM and Fatichi S 2017 Linking plant functional trait plasticity and the large increase in forest water use efficiency *Journal of Geophysical Research: Biogeosciences* **122** 2393–2408

McCarroll D and Loader NJ 2004 Stable isotopes in tree rings *Quaternary Science Reviews* **23** 771-801

McDonald PM 1983 Local volume tables for Pacific madrone, tanoak, and California black oak in north-central California *Pacific Southwest Forest and Range Experiment Station Research Note PSW-362* (Forest Service, Berkeley, CA, USA)

Medlyn BE *et al* 2017 How do leaf and ecosystem measures of water-use efficiency compare? *New Phytologist* **216** 758-777

Michelot A, Eglin T, Dufrêne E, Lelarge-Trouverie C and Damesin C 2011 Comparison of seasonal variations in wateruse efficiency calculated from the carbon isotope

composition of tree rings and flux data in a temperate forest *Plant, Cell & Environment* **34** 230–44

Mote PW, Hamlet AF, Clark MP and Lettenmaier DP 2005 Declining mountain snow pack in western North America *Bull. Am. Met. Soc.* **86** 39-49

Norby RJ and Luo YQ 2004 Evaluating ecosystem responses to rising atmospheric CO_2 and global warming in a multi-factor world *New Phytologist* **162** 281–293

Oren R, Sperry JS, Katul GG, Pataki DE, Ewers BE, Phillips N and Shafer KV 1999 Survey and synthesis of intra- and interspecific variation in stomatal sensitivity to vapour pressure deficit *Plant, Cell & Environment* **22** 1515-1526

Pan Y *et al* 2011 A large and persistent carbon sink in the world's forests *Science* **333** 10.1126/science.1201609

Perez-Priego O, Katul G, Reichstein M, El-Madany TS, Ahrens B, Carrara A, Scanlon TM and Migliavacca M 2018 Partitioning eddy covariance water flux components using physiological and micrometeorological approaches *Journal of Geophysical Research:Biogeosciences* **123** 3353-3370

Pinheiro J, Bates D and R Core Team 2015 nlme: Linear and Nonlinear Mixed Effects Models. R package version 3.1-121 (http://CRAN.R-project.org/package=nlme)

Pile LS, Meyer MD, Rojas R, Roe O and Smith MT 2019 Drought Impacts and Compounding Mortality on Forest Trees in the Southern Sierra Nevada *Forests* **10** 237

Reichstein M *et al* 2013 Climate extremes and the carbon cycle *Nature* **500** 10.1038/nature12350

Reichstein M *et al* 2007 Reduction of ecosystem productivity and respiration during the European summer 2003 climate anomaly: a joint flux tower, remote sensing and modelling analysis *Global Change Biology* **13** 634-51

Reichstein M, Tenhunen JD, Roupsard O, Ourcival JM, Rambal S, Miglietta F, Peressotti A, Pecchiari M, Tirone G and Valentini R 2002 Severe drought effects on ecosystem CO_2 and H_2O fluxes at three Mediterranean evergreen sites: revision of current hypotheses? *Global Change Biology* **8** 999-1017

Rocha AV, Goulden ML, Dunn AL and Wofsy SC 2006 On linking interannual tree ring variability with observations of whole-forest CO_2 flux *Glob. Change Biol.* **12** 1378–89

Roden JS and Ehleringer JR 2007 Summer precipitation influences the stable oxygen and carbon isotopic composition of tree-ring cellulose in Pinus ponderosa *Tree Physiology* **27** 491-501

Saurer M *et al* 2014 Spatial variability and temporal trends in water-use efficiency of European forests *Global Change Biology* **20** 3700-3712

Schimel D, Pavlick R, Fisher JB, Asner GP, Saatchi S, Townsend P, Miller C, Frankenberg C, Hibbard K and Cox P 2015 Observing terrestrial ecosystems and the carbon cycle from space *Glob Change Biology* **21** 1762-1776

Schwartz M, Hall A, Sun F, Walton D and Berg N 2017 Significant and inevitable end-of-twenty-first-century advances in surface runoff timing in California's Sierra Nevada *Journal of Hydrometeorology* **18** 3181-97

Shukla S, Safeeq M, AghaKouchak A, Guan K and Funk C 2015 Temperature impacts on the water year 2014 drought in California *Geophysical Research Lett*ers **42** 4384–4393

Stewart I, Cayan DC and Dettinger MD 2004 Changes in snowmelt runoff timing in Western North America under a 'business as usual' climate change scenario *Climatic Change* **62** 217–232

Stoy PC *et al* 2019 Reviews and syntheses: Turning the challenges of partitioning ecosystem evaporation and transpiration into opportunities *Biogeosciences Discussions* 10.5194/bg-2019-85

Still CJ *et al* 2009 Influence of clouds and diffuse radiation on ecosystem-atmosphere CO_2 and $CO^{18}O$ exchanges *Journal of Geophysical Research: Biogeosciences* **114** 10.1029/2007JG000675

Teets A, Fraver S, Hollinger DY, Weiskittel AR, Seymour RS and Richardson AD 2018 Linking annual tree growth with eddy-flux measures of net ecosystem productivity across twenty years of observation in a mixed conifer forest. *Agric. For. Meteorol.* **249** 479–487

Tei S, Sugimoto A, Kotani A, Ohta T, Morozumi T, Saito S, Hashiguchi S and Maximov T 2019 Strong and stable relationships between tree-ring parameters and forest-

level carbon fluxes in a Siberian larch forest *Polar Science* (Accepted manuscript) https://doi.org/10.1016/j.polar.2019.02.001

Thomas RB, Spal SE, Smith KR and Nippert JB 2013 Evidence of recovery of Juniperus virginiana trees from sulfur pollution after the Clean Air Act *PNAS USA* **110** 15319–15324

Voelker SL, Meinzer FC, Lachenbruch B, Brooks JR and Guyette RP 2014 Drivers of radial growth and carbon isotope discrimination of bur oak (*Quercus macrocarpa* Michx.) across continental gradients in precipitation, vapour pressure deficit and irradiance *Plant, Cell & Environment* **37** 766-79

Voelker SL, Muzika RM, Guyette RP and Stambaugh MC 2006 Historical CO_2 growth enhancement declines with age in Quercus and Pinus *Ecological Monographs* **76** 549–564

Voelker SL *et al* 2016 A dynamic leaf gas-exchange strategy is conserved in woody plants under changing ambient CO_2: evidence from carbon isotope discrimination in paleo and CO_2 enrichment studies *Global Change Biology* **22** 889-902

Voelker SL, Merschel AG, Meinzer FC, Ulrich DE, Spies TA and Still CJ 2018 Fire deficits have increased drought sensitivity in dry conifer forests: Fire frequency and tree-ring carbon isotope evidence from Central Oregon *Global Change Biology* **25** 10.1111/gcb.14543

Voelker SL 2011 Age-dependent changes in environmental influences on tree growth and their implications for forest responses to climate change *Size- and Age-related*

Changes in Tree Structure and Function ed Meinzer F, Lachenbruch B and Dawson T (Dorderect: Springer) pp 455-479

Voelker SL, Wang S.-Y, Dawson TE, Roden JS, Still CJ, Longstaffe FJ and Ayalon A 2019 Tree-ring isotopes adjacent to Lake Superior reveal cold winter anomalies for the Great Lakes region of North America *Scientific Reports* **9** 4412

Westerling AL, Hidalgo HG, Cayan DR and Swetnam TW 2006 Warming and earlier spring increase western US forest wildfire activity *Science* **313** 940–943

Yang YT, Long D and Shang SH 2013 Remote estimation of terrestrial evapotranspiration without using meteorological data *Geophysical Research Letters* **40** 3026–3030

Yi K, Maxwell JT, Wenzel MK, Roman DT, Sauer PE, Phillips RP and Novick KA 2019 Linking variation in intrinsic water-use efficiency to isohydricity: a comparison at multiple spatiotemporal scales *New Phytologist* **221** 195-208

Yoon J-H, Wang S-Y, Gillies RR, Kravitz B, Hipps L and Rasch PJ 2015 Increasing water cycle extremes in California and in relation to ENSO cycle under global warming *Nature Communication* **6** 10.1038/ncomms9657

Zhang BC, Cau JJ, Bai YF, Yang SJ, Hu L and Ning ZG 2011 Effects of cloudiness on carbon dioxide exchange over an irrigated maize cropland in northwestern China *Biogeosciences* **8** 1669-1691

Zhao L, Li YN, Gu S, Zhao XQ, Xu SX and Yu GR 2005 Carbon dioxide exchange between the atmosphere and an alpine shrubland meadow during the growing

season on the Qinghai-Tibetan Plateau *Journal of Integrated Plant Biology* **47** 271–282

Zhou S, Yu B, Huang Y and Wang G 2014 Daily underlying water use efficiency for AmeriFlux sites *Journal of Geophysical Research: Biogeosciences* **120** 887-902

Zhou S, Zhang Y, Williams AP and Gentine P 2019 Projected increases in intensity, frequency, and terrestrial carbon costs of compound drought and aridity events *Science Advances* **5** eaau5740

Tables and Figures

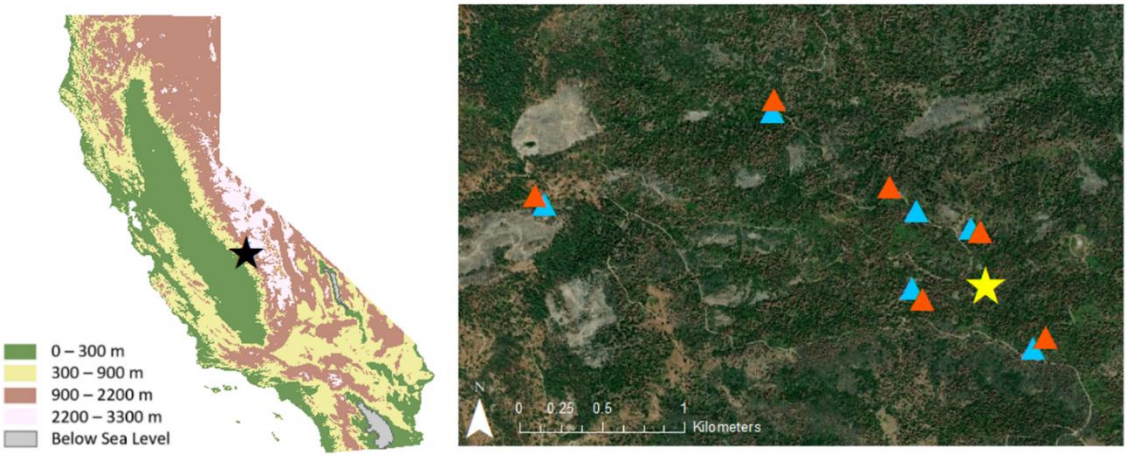

Figure 3-1. Location of the Soaproot Saddle field site (black star) in central California (37.03N, 119.25W) (left panel). Plot and flux tower locations at Soaproot Saddle (right panel). Blue triangles represent plots with surviving focus trees, red triangles represent plots with dead focus trees. Surviving and dead focus tree plots in close proximity are paired trees. The yellow star represents the location of the Soaproot Saddle SSCZO flux tower.

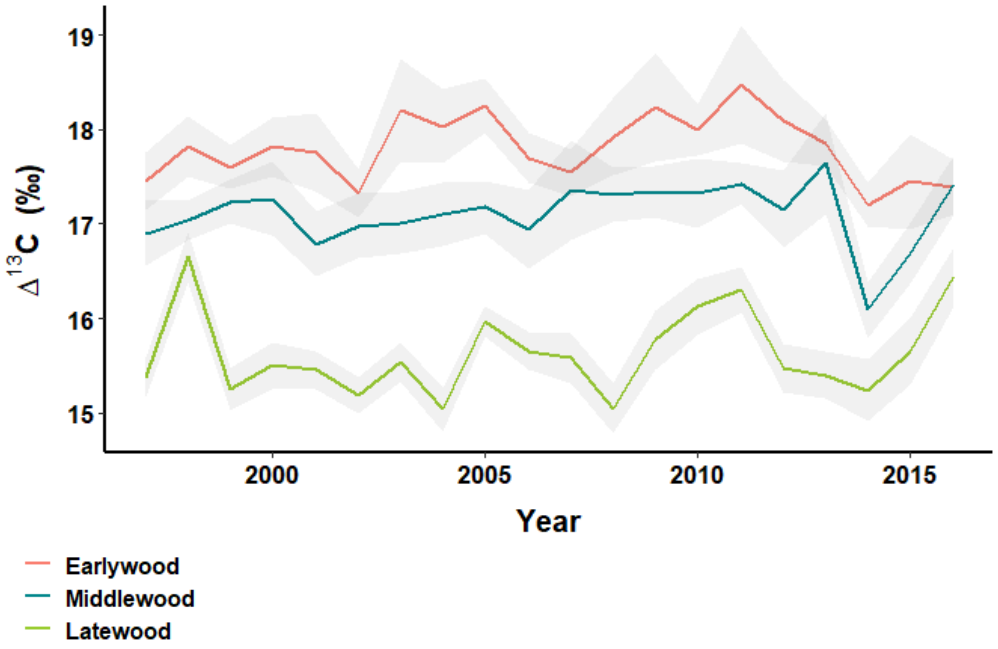

Figure 3-2. Pre-whitened earlywood (red), middlewood (blue), and latewood (green) $\Delta^{13}C$ for the years 1997-2016.

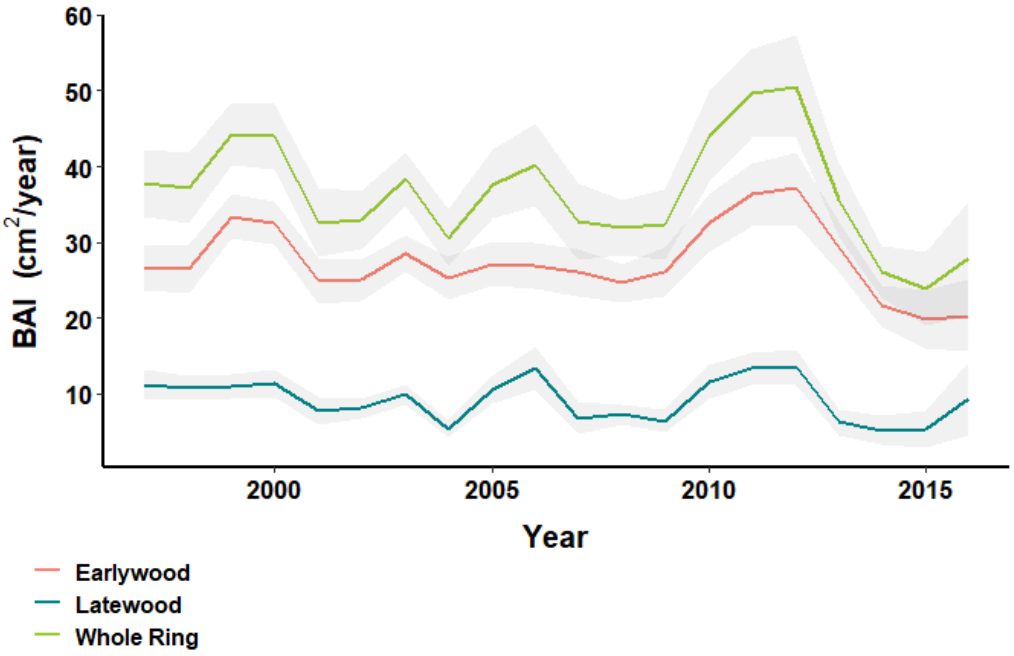

Figure 3-3. Whole-ring (green), earlywood (red), and latewood (blue) BAI for the years 1997-2016.

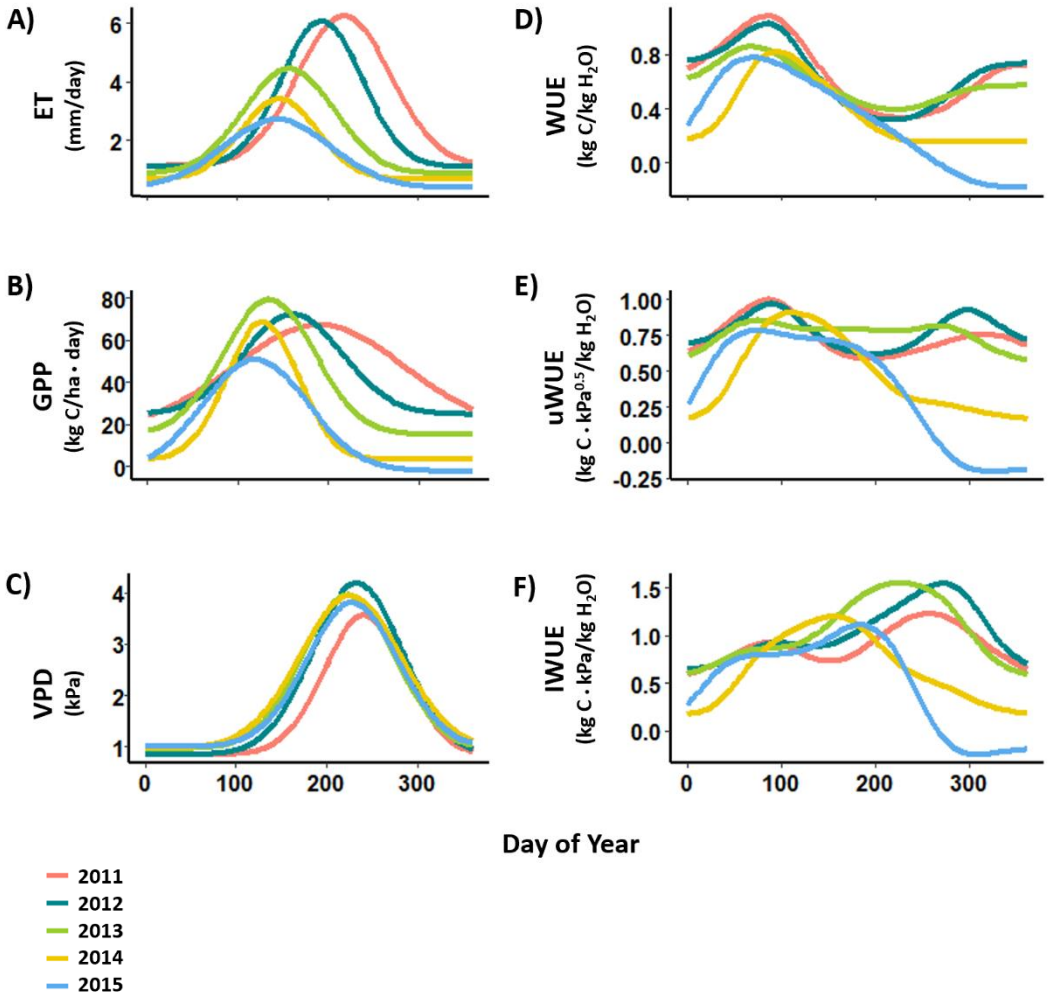

Figure 3-4. Interpolated estimates for evapotranspiration (ET; A), gross primary productivity (GPP; B) and vapor pressure deficit (VPD; C) and associated calculations of WUE (D), uWUE (E), and IWUE (F) by day of year for each year from 2011-2015. Curves for ET, CO_2 flux and VPD were estimated based on Gaussian curves fit to monthly-resolution data.

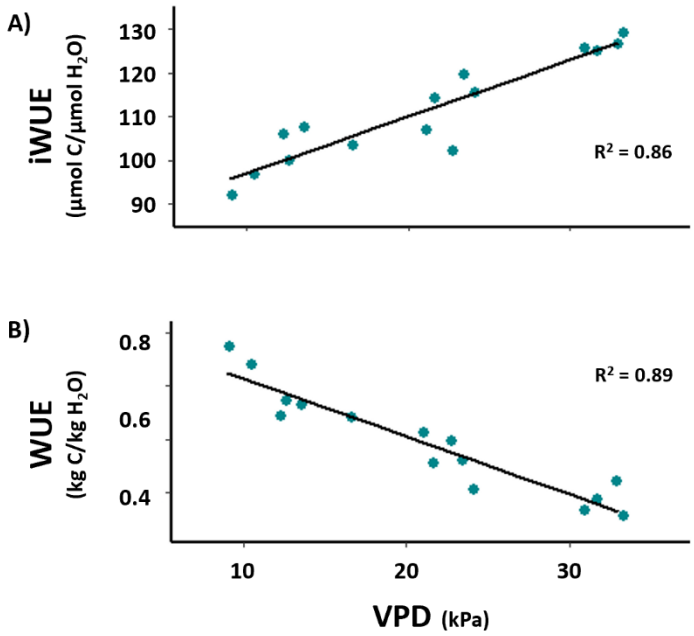

Figure 3-5. Regression analysis for VPD and iWUE (A) and ecosystem-scale WUE (B) for the years 2011-2015. iWUE derived from earlywood was compared to spring VPD (Mar, Apr, May), iWUE derived from latewood was compared to summer (Jun, Jul, Aug), and iWUE derived from middlewood was compared to the average of spring and summer VPD. Both regression analyses were significant ($p < 0.01$ in both cases).

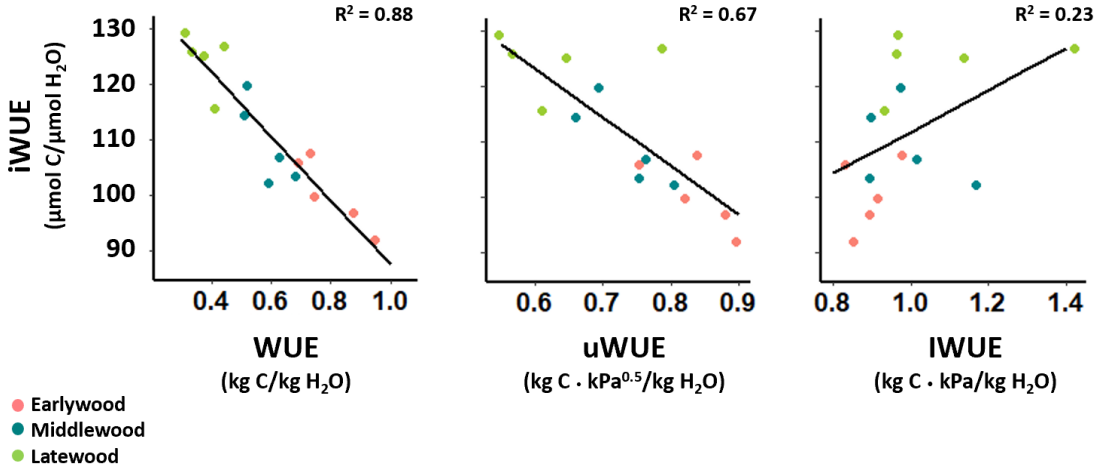

Figure 3-6. Regression analysis for iWUE and WUE (A), uWUE (B), and IWUE (C) for the years 2011-2015. Colors represent seasonal windows corresponding to early-, middle- and latewood formation. Regression analyses including WUE (A) and uWUE (B) were significant ($p < 0.01$ in both cases), but the regression analysis for iWUE and IWUE was not ($p = 0.07$).

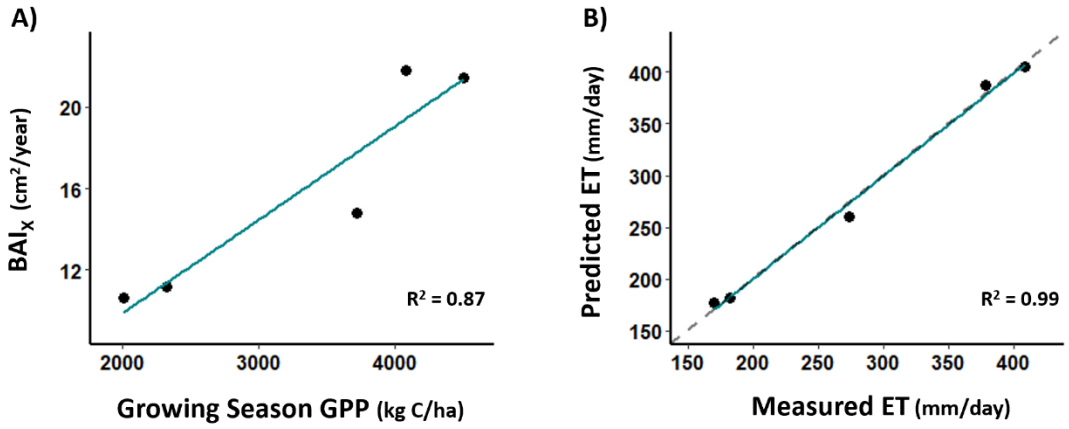

Figure 3-7. Regression analysis for BAI_x values and growing season (March – October) ecosystem GPP ($p < 0.001$) (A) and the final relationship between measured and predicted ET ($p < 0.01$) (B). ET was estimated by dividing BAI_x values by iWUE, performing a regression analysis of measured ET versus this ratio of BAI_x/iWUE that can be described by the equation ET = 2043.6 (BAI_x/iWUE) – 6.119. This equation was used to predict ecosystem-scale ET, shown in panel B. Dashed grey line in panel B represents a 1:1 relationship.

CHAPTER 4

SUMMARY AND CONCLUSIONS

Climate warming in recent decades has resulted in more frequent and severe drought events, intensified drought-associated disturbances, and increased hydrological extremes in California. All of these changes provide challenges for forests in California and across the western United States. The 2012-2015 California drought (hereafter referred to as the "CA Drought") was particularly severe and led to an epidemic-scale outbreak of western pine beetle in the central and southern portions of the Sierra Nevadas. The result was widespread mortality of dominant canopy tree species, including ponderosa pine, across much of this region. The likelihood of such events is projected to increase, making unprecedented events associated with the CA Drought and beetle outbreak more likely. The importance of these forests to local economies and ecosystem services critical to California makes it important for us to gain a better understanding of how these situations may be avoided in the future. A more basic and essential question that can inform management decisions for this region in the future is: Why do trees die during these events, and which trees have the best chance of survival? This question encompasses stand-scale aspects, including stand density, competition, and host tree abundance, as well as individual-scale aspects, including tree physiology and strategies for resources allocation. In this study, we were interested in both the stand-scale and individual-scale influences on ponderosa pine responses to the CA Drought.

In chapter 2, we compared surviving and dead ponderosa pines following the CA Drought to determine whether differences existed between the two groups that could explain why some of these trees managed to survive. We expected to see evidence of greater drought stress in trees that died, which would have indicated that drought stress increased susceptibility to bark beetle attacks. However, there was no evidence of differences in severity of drought stress in the absolute values or climate sensitivity of tree-ring stable isotope records. Our results suggest that survival was strongly associated with greater growth, likely due to genetic differences in phenological timing, as well as relative isolation from conspecific host trees that could have provided a buffer from intensity of bark beetle attack.

In chapter 3, we investigated how tree-level responses to severe drought (particularly iWUE and growth rates) compared to ecosystem-level responses (WUE, GPP, and ET). Comparisons of these types of data have been rare and fraught with difficulties because tree-ring isotopes record individual overstory tree responses to climate, whereas flux towers record fluxes from all vegetation, as well as soil and surface water, within the tower footprint. In the case of Soaproot Saddle, flux measurements include evaporation of soil moisture and stream water from a portion of Big Creek. We found that iWUE and WUE had opposite relationships with vapor pressure deficit, clearly indicating that there were stark differences in measures of water use efficiency that were being recorded at these two scales. Nonetheless, a strong negative relationship between iWUE and WUE, as well as a strong positive relationship between growth rates and ecosystem-scale GPP, allowed us to retrodict ecosystem-scale ET at Soaproot Saddle

during the CA Drought event using tree-ring measurements. Our results showed that, although tree- and ecosystem-scale water use efficiency had diverging responses to VPD and to each other, tree-level measurements were still successful proxies for ecosystem-scale carbon and water fluxes at this site. The combined use of tree-ring growth and carbon isotope measurements have great potential to improve our ability to estimate ecosystem-scale carbon and water fluxes in areas where flux towers are not present, and to reconstruct those fluxes back in time.

Overall, these studies allowed us to explore ponderosa pine responses to severe drought stress during the CA Drought and associated western pine beetle outbreak. We found that, for the large ponderosa pines sampled in this study, growth rates had the most influence on survival as opposed to severity of drought stress. We also found that ponderosa pine tree-ring stable isotopes and growth rates recorded important ecosystem carbon and water flux signals during this drought event. Understanding the physiological responses of trees to extreme drought, as well as the relationship between drought stress and susceptibility to disturbance events, can give us more insight for managing at-risk forests in California and across the western United States. Since many of these forests include economically and ecologically important tree species (including ponderosa pine), future mortality events of this scale could have major consequences for California's tourism economy, timber production, forest biodiversity, and water quality. A better understanding of how trees respond to and record severe drought events will allow us to better predict, and hopefully mitigate, future forest mortality events in California and across the western United States.

APPENDICES

APPENDIX A

CHAPTER 2 SUPPLEMENTARY FIGURES AND TABLES

Table A-1 DBH measurements and ages of the randomly sampled trees collected by Ferrell (2017).

	Mean	**SD**	**N**
DBH (cm)	47.27	16.18	43
Age	117.84	41.61	43

Table A-2 P-values corresponding with Pearson's correlation coefficients in Table 2-2. P-values < 0.05 are denoted by (**) and p-values < 0.1 are denoted by (•).

A) $\Delta^{13}C$

	Surviving Focus Trees				*Dead Focus Trees*			
	Winter	**Spring**	**Summer**	**Fall**	**Winter**	**Spring**	**Summer**	**Fall**
PDSI	**< 0.01****	**< 0.01****	**< 0.01****	**< 0.01****	**< 0.01****	**< 0.01****	**< 0.01****	**< 0.01****
VPD	0.12	**< 0.01****	**< 0.01****	0.22	**< 0.01****	**< 0.01****	**< 0.01****	0.14
CMD	0.81	**< 0.01****	**< 0.01****	**0.09•**	0.22	**< 0.01****	**< 0.01****	0.42
Precip	**0.03****	**< 0.01****	**0.09•**	0.75	**< 0.01****	**< 0.01****	**0.02****	0.75

B) $\delta^{18}O$

	Winter	**Spring**	**Summer**	**Fall**	**Winter**	**Spring**	**Summer**	**Fall**
PDSI	0.63	0.69	0.63	0.75	**0.09•**	**0.03****	**0.01****	0.12
VPD	0.57	0.75	0.47	0.63	0.29	0.17	0.75	0.47
CMD	**0.07•**	0.75	0.69	0.22	0.25	0.25	0.69	**0.07•**
Precip	0.57	0.57	0.87	0.52	0.87	0.19	0.69	**0.09•**

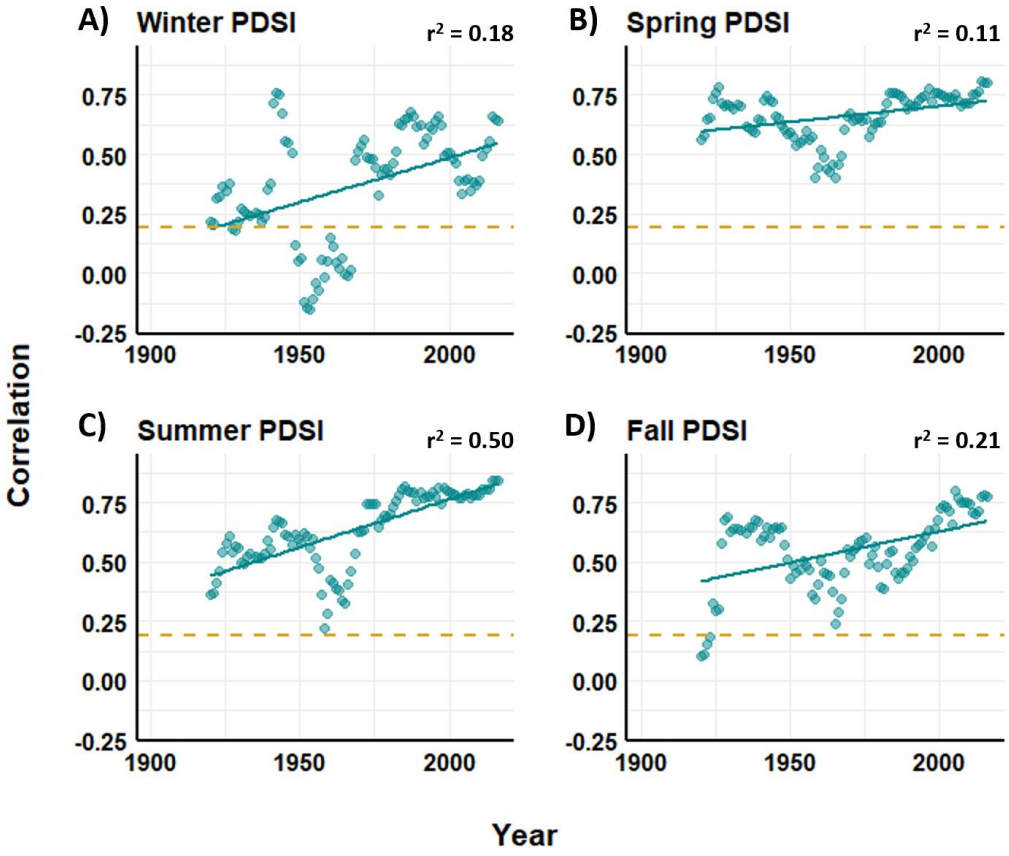

Figure A-1 20-year moving window correlations for $\Delta^{13}C$ and (A) winter PDSI (December-February), (B) spring PDSI (March-May), (C) summer PDSI (June-August), and (D) fall PDSI (September-November). Pre-whitened isotope data (including surviving and dead focus trees) was compared to residual climate data for the years 1900-2016. Linear trendlines were fit to each plot and r^2 values are included in each panel. Yellow dashed lines represent the correlation significance cutoff – significant correlations are ≥ 0.19 or ≤ -0.19.

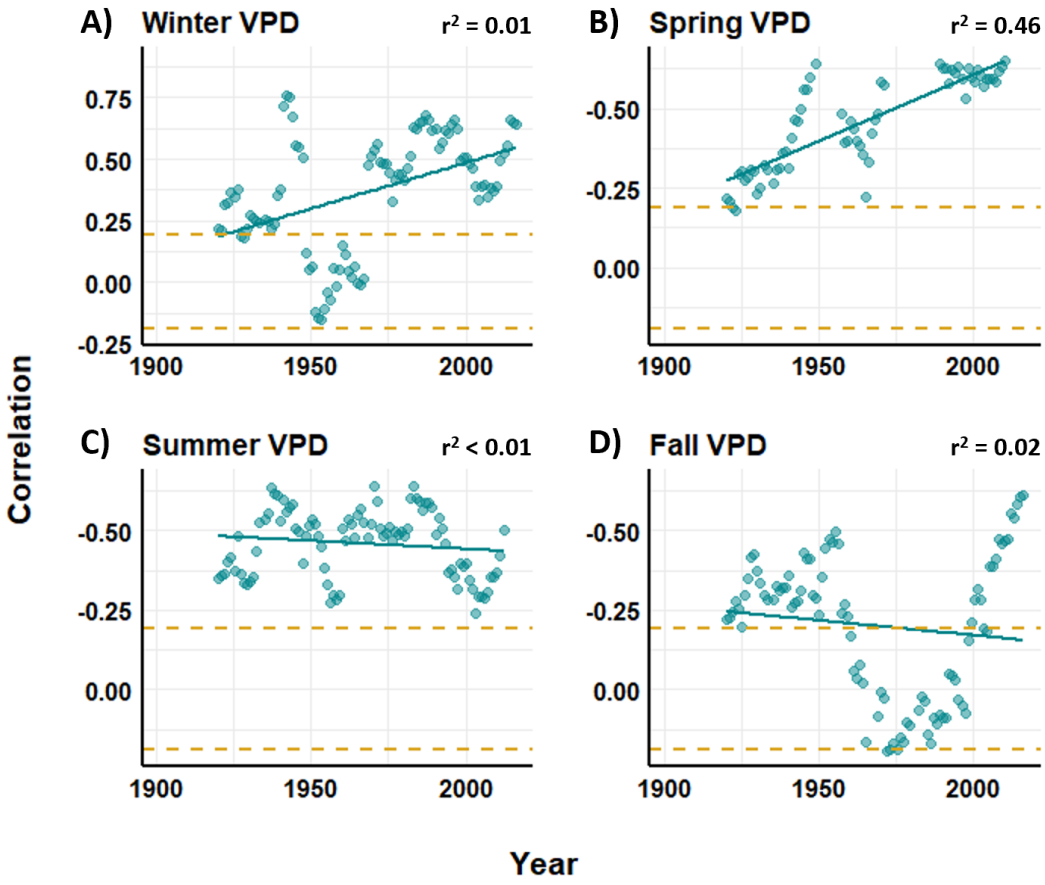

Figure A-2 20-year moving window correlations for $\Delta^{13}C$ and (A) winter VPD (December-February), (B) spring VPD (March-May), (C) summer VPD (June-August), and (D) fall VPD (September-November). Pre-whitened isotope data (including surviving and dead focus trees) was compared to residual climate data for the years 1900-2016. Linear trendlines were fit to each plot and r^2 values are included in each panel. Yellow dashed lines represent the correlation significance cutoff – significant correlations are ≥ 0.19 or ≤ -0.19.

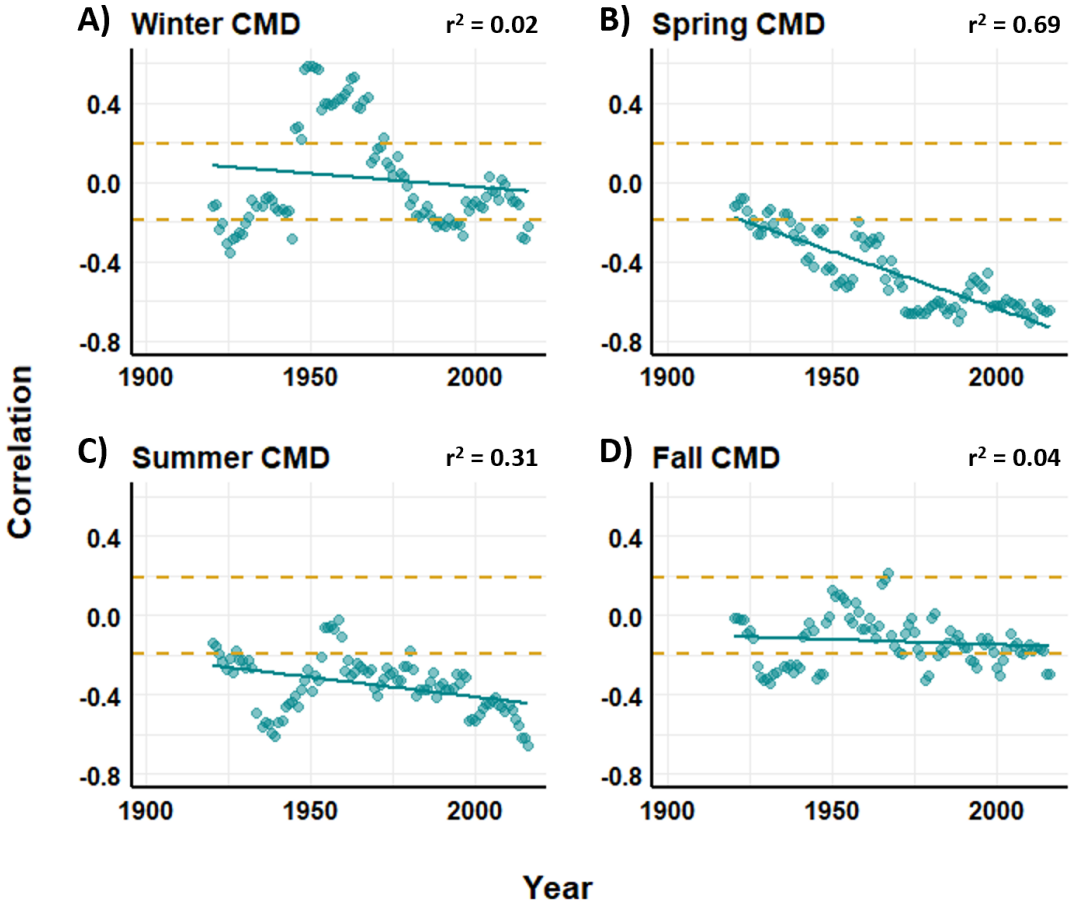

Figure A-3 20-year moving window correlations for $\Delta^{13}C$ and (A) winter CMD (December-February), (B) spring CMD (March-May), (C) summer CMD (June-August), and (D) fall CMD (September-November). Pre-whitened isotope data (including surviving and dead focus trees) was compared to residual climate data for the years 1900-2016. Linear trendlines were fit to each plot and r^2 values are included in each panel. Yellow dashed lines represent the correlation significance cutoff – significant correlations are ≥ 0.19 or ≤ -0.19.

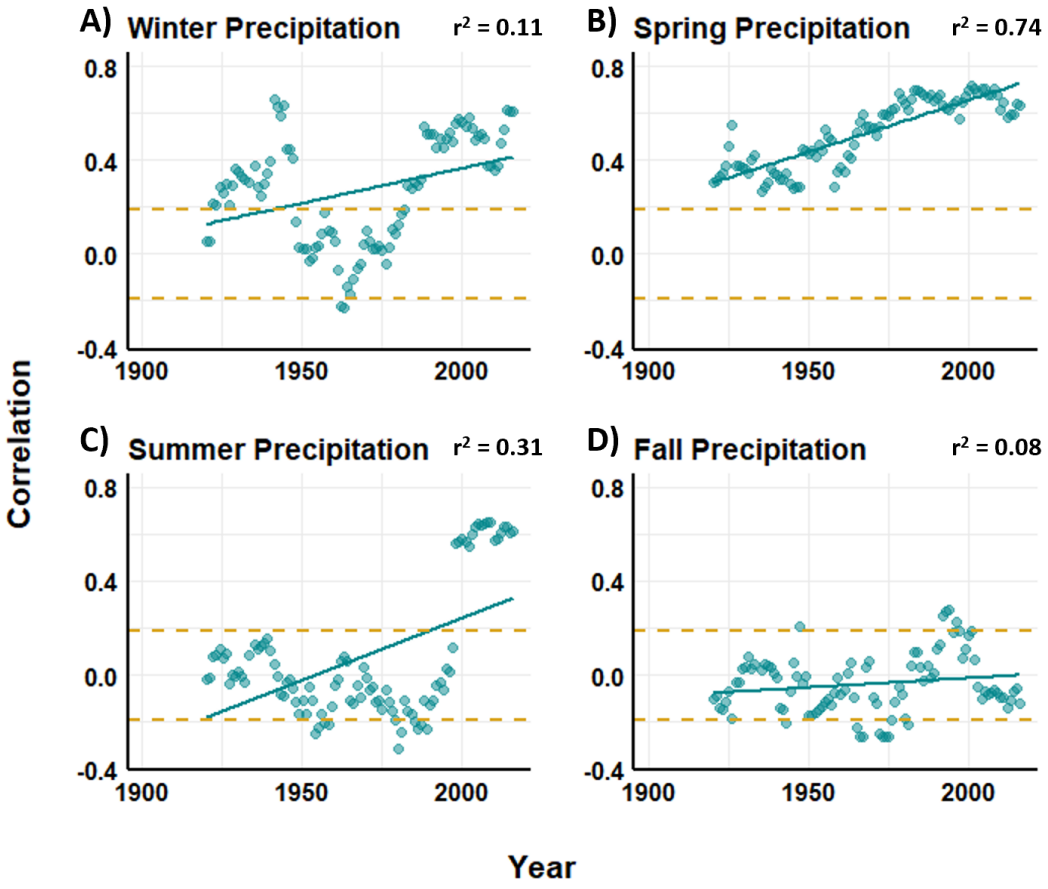

Figure A-4 20-year moving window correlations for $\Delta^{13}C$ and (A) winter precipitation (December-February), (B) spring precipitation (March-May), (C) summer precipitation (June-August), and (D) fall precipitation (September-November). Pre-whitened isotope data (including surviving and dead focus trees) was compared to residual climate data for the years 1900-2016. Linear trendlines were fit to each plot and r^2 values are included in each panel. Yellow dashed lines represent the correlation significance cutoff – significant correlations are ≥ 0.19 or ≤ -0.19.

APPENDIX B

CHAPTER 3 SUPPLEMENTARY FIGURES AND TABLES

Table B-1 Supporting data for figure 3-5, including year and ring portion or season. Earlywood iWUE values correspond with spring WUE and VPD (March-May), latewood iWUE values correspond with summer WUE and VPD (June-August), and middlewood iWUE values correspond with the average of spring and summer WUE and VPD values (March-August).

	Year	iWUE (µmol C/µmol H_2O)	WUE (kg C/kg H_2O)	VPD (kPa)
Earlywood	2011	92.09	0.95	9.14
	2012	96.78	0.88	10.55
	2013	99.88	0.74	12.65
	2014	107.62	0.73	13.63
	2015	105.89	0.69	12.34
Middlewood	2011	103.4	0.68	16.63
	2012	106.92	0.63	21.12
	2013	102.24	0.59	22.8
	2014	119.8	0.52	23.48
	2015	114.31	0.51	21.64
Latewood	2011	115.52	0.41	24.12
	2012	125.15	0.37	31.69
	2013	126.67	0.44	32.94
	2014	129.16	0.31	33.33
	2015	125.75	0.33	30.94

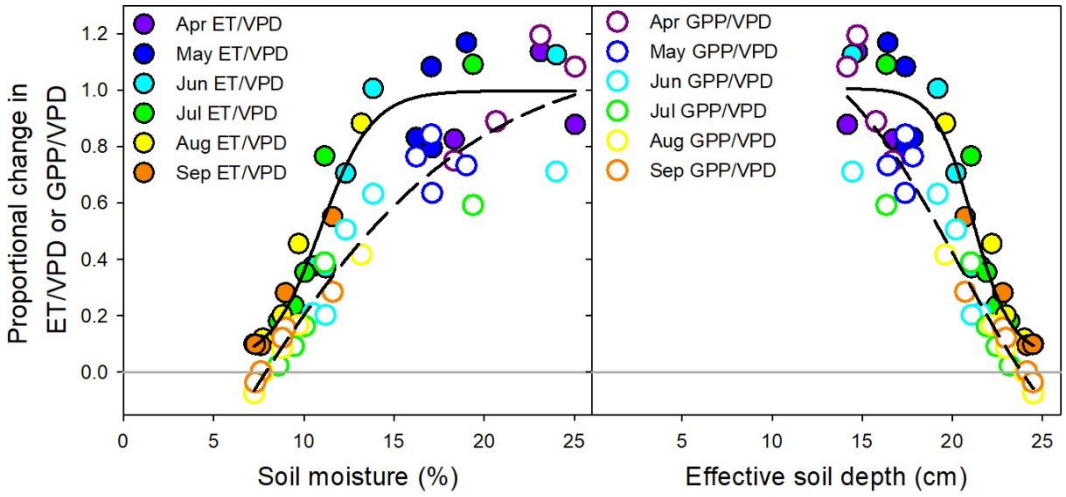

Figure B-1 Ratios of ET/VPD and GPP/VPD compared to (A) soil moisture content measured using a cosmic ray soil moisture sensor near the Soaproot Saddle flux tower and (B) soil effective depth for the years 2011-2015. Flux tower measurements of monthly (April-September) ET and GPP for these years were divided by VPD to remove the effect of monthly variations in VPD. Ratios of ET/VPD (closed circles, solid line) and GPP/VPD (open circles, dashed line) were compared to soil moisture content (%) and effective soil depth (cm), then scaled to be proportional to the predicted maximum value at the highest soil moisture content or effective soil depth for each month. Proportional ET/VPD and GPP/VPD values were then plotted against soil moisture content and effective soil depth for each month during the years 2011-2015 to observe the different responses of ET and GPP to progressive soil drying at Soaproot Saddle.